



Numerical simulation of urban impact on precipitation in Tokyo: How does urban temperature rise affect precipitation?



Naoko Seino ^{*}, Toshinori Aoyagi, Hiroshige Tsuguti

Meteorological Research Institute, 1-1 Nagamine Tsukuba, Ibaraki 305-0052, Japan

ARTICLE INFO

Article history:

Received 31 May 2016

Received in revised form 21 November 2016

Accepted 22 November 2016

Keywords:

Urban impact on precipitation

Numerical simulation

Urban canopy scheme

Urban heat island

Tokyo

Precipitation variability

ABSTRACT

This study explored how heat island intensification affects precipitation in the Tokyo metropolitan area. Numerical experiments were made for the month of August from 2006 to 2013 using the Non-Hydrostatic Model (NHM) with a horizontal grid interval of 2 km and the Square Prism Urban Canopy (SPUC) scheme. We performed the experiments with two different specifications for the Tokyo area: the current highly urbanized surface conditions (CRNT experiment) and less urbanized conditions (MDUB experiment). The simulation results suggest that the mean monthly precipitation in the central Tokyo area was approximately 10% larger in the CRNT experiment than in the MDUB experiment, associated with a mean temperature rise of as much as 1 °C. We also examined the modification of daily precipitation characteristics in the two experiments. The CRNT experiment generally yielded larger amounts of area-maximum precipitation in the urban domain; however, differences between the experiments in daily precipitation varied among cases. Composite analysis was performed to investigate the processes associated with the differences in simulated precipitation. We found that in afternoon rainfall cases without preceding precipitation, a thermally induced change in circulation, particularly enhanced ascending motion, played an important role in the precipitation increase in the CRNT experiment.

© 2016 Elsevier B.V. All rights reserved.

1. Introduction

Evaluating the impact of urbanization on precipitation is an important problem in urban climate research. Precipitation variability is critical for water resource management in and around urban areas, and estimates of

* Corresponding author.

E-mail addresses: nseino@mri-jma.go.jp (N. Seino), taoyagi@mri-jma.go.jp (T. Aoyagi), htsuguti@mri-jma.go.jp (H. Tsuguti)

precipitation modification in urban areas, particularly for heavy rainfall, are necessary for disaster preparedness. Urban climate in the Tokyo metropolitan area, an agglomeration of 38 million inhabitants (United Nations, 2014), has long been studied using various approaches (Fujibe, 2011, 2012), but the urban influence on precipitation in this area is still not fully understood. The Tokyo metropolitan area is on the southeastern coast of central Japan and usually has an abundant moisture supply. Temporal and spatial variations in precipitation depend predominantly on the activities and tracks of mid-latitude disturbances and tropical cyclones, which means that an urban effect is not easily detected in long-term observation data.

Yonetani (1982, 1989) pioneered research on the urban influence on precipitation variability at Tokyo. Kanae et al. (2004) analyzed Tokyo precipitation records from 1890 to 1999 and showed that hourly heavy precipitation in the 1990s was not unprecedented in strength or frequency. Fujibe et al. (2009) investigated hourly precipitation data from the same station for a longer period (1890–2007) and the Automated Meteorological Data Acquisition System (AMeDAS) data from surrounding stations for the most recent 30 years. They found that “no preceding precipitation” (NPP) cases showed both an increasing trend at a rate of 30%/century or more and a positive spatial anomaly in Tokyo between afternoon and early evening in the warm season. Although increases in heavy rainfall have been detected at many other stations in less urbanized parts of Japan (Fujibe et al., 2005; Japan Meteorological Agency, 2014), Inoue and Kimura (2004, 2007) used satellite imagery to show that cumulus formation was enhanced in the Tokyo area in the warm season. Moreover, Sato et al. (2006) and Takahashi et al. (2011) suggested an enhancement of precipitation over or downwind of the most urbanized parts of Tokyo. These observation-based findings suggest the possibility of an urban effect on the increase of warm-season short-term precipitation in Tokyo.

The urban effect on precipitation has been investigated for many cities (Shepherd, 2005; Kanda, 2007; Pielke et al., 2007; Shepherd, 2013; Han et al., 2014; Mitra and Shepherd, 2016), particularly in the United States, with an emphasis on convective precipitation. METROMEX was the first major field program to investigate the existence and causes of urban rainfall anomalies that had been suggested in several previous climatological studies (Changnon, 1981). Changnon et al. (1976) used METROMEX data to infer statistically significant increases in summer rainfall and thunderstorms in and just downwind of St. Louis, Missouri. Subsequent studies have suggested various kinds of urban impacts, such as the enhancement of precipitation around urban areas, based on observations (Kishtawal et al., 2010; Kug and Ahn, 2013), changes in diurnal precipitation patterns (Balling and Brazel, 1987), urban-induced rainfall (Bornstein and Lin, 2000; Dixon and Mote, 2003), precipitation increases downwind of urban areas (Shepherd et al., 2002; Mote et al., 2007; Hand and Shepherd, 2009), and spatial rainfall modifications, including storm splitting (Niyogi et al., 2011). Ashley et al. (2012) demonstrated positive urban amplification of thunderstorm frequency and intensity for major cities in the Southeast United States by using radar reflectivity and lightning data. Results of Haberlie et al. (2015) revealed that isolated convective initiation (ICI) events occurred more often over the urban area compared to its surrounding rural counterparts. Meanwhile, some studies have documented decreases in rainfall due to urbanization (Rosenfeld, 2000; Kaufmann et al., 2007). Changnon (2001) confirmed that the net urban effect was an increase in storm activity over the central part of Chicago and suggested that urban complexes of more than three million inhabitants are likely to have locally altered storm activity. The variety of precipitation responses revealed by these studies shows that urban effects on precipitation are quite complex and dependent on many factors including city size, surrounding land use, water cycles, and regional climate. Mitra and Shepherd (2016) states that complex urban land-atmospheric interactions are not easy to grasp and more research must be done to understand the impact of morphology, shape, aerosols and microscale temperature patterns on urban precipitation variability.

Numerical simulations are useful for analyzing and quantifying urban processes, and the number of numerical experiments has grown in recent years (e.g., Baik et al., 2001; Rozoff et al., 2003; Gero and Pitman, 2006; Niyogi et al., 2006, 2011; Shem and Shepherd, 2009). Trusilova et al. (2008) and Hamdi et al. (2012) showed that inclusion of urban land cover resulted in an increase of winter precipitation and a reduction of summer precipitation in Europe. Numerical investigations have also addressed urban effects on precipitation in Asian cities (Lin et al., 2008; Zhang et al., 2009; Wang et al., 2012; Yang et al., 2014; Zhang et al., 2014), and several have been carried out for cases involving rainfall in Tokyo.

Matheson and Ashie (2008) modeled the effect of land surface changes in Tokyo for two selected rainfall cases and showed that the presence of urban land use types enhanced rainfall in one case and slightly reduced it in the other case. Shimizu et al. (2010) showed that urbanization in Tokyo apparently increased rainfall in five of nine localized heavy rain events and decreased it or had no effect in the other four cases. Ikeuchi et al. (2007) found that changes in urban distribution and anthropogenic heat output greatly affected the positions

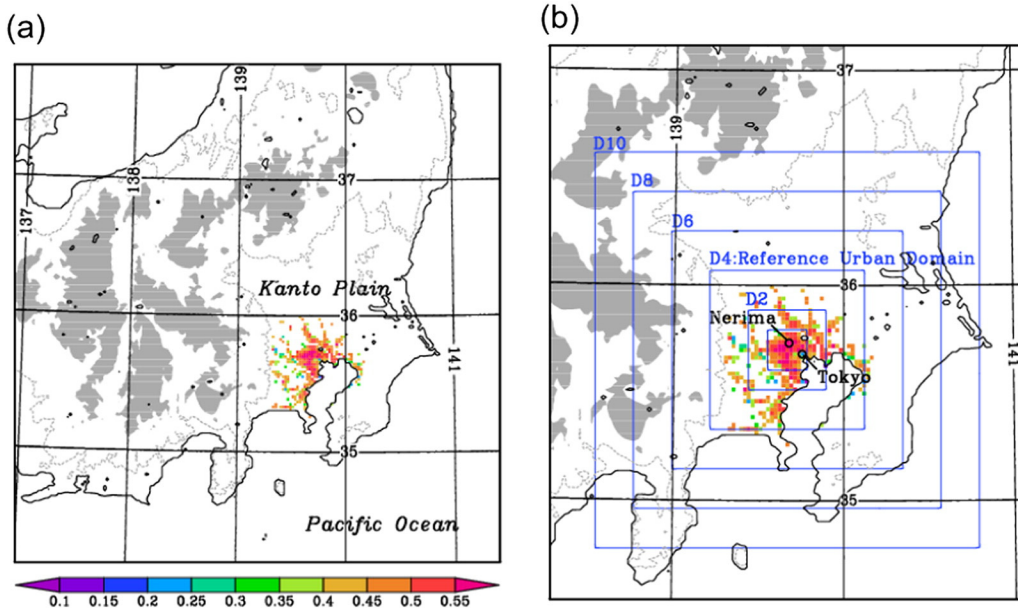


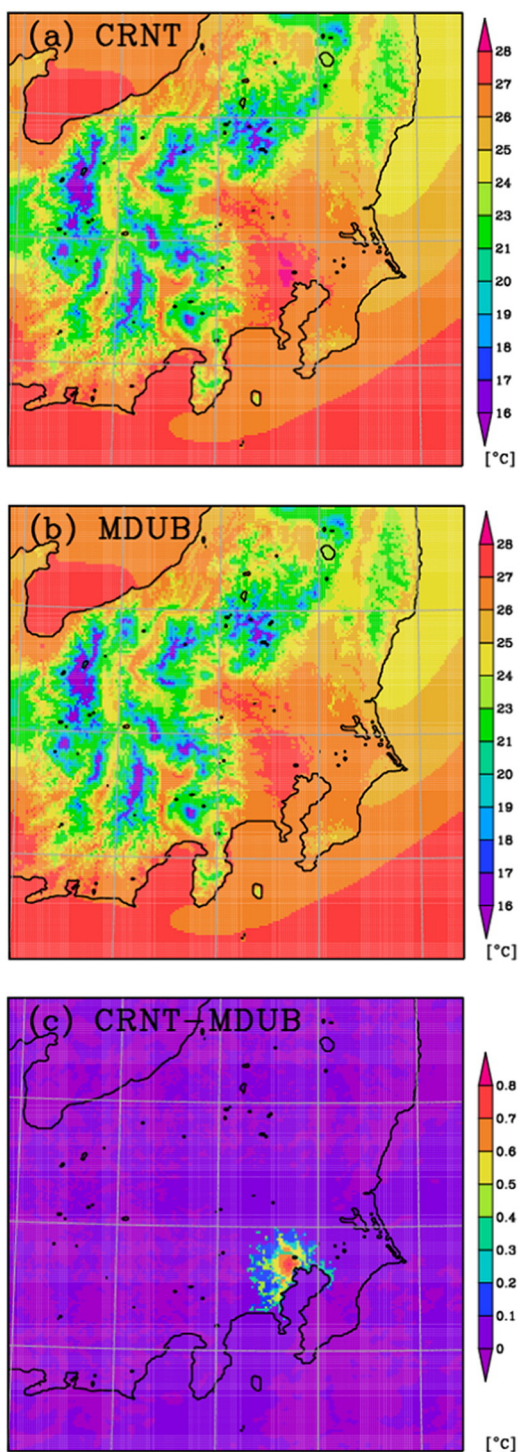
Fig. 1. Location maps showing (a) the model domain of NHM and (b) the Kanto Plain area. Colors denote the building fraction of grid cells to which SPUC was applied. Dotted gray lines are the 200-m topographic contour, and gray shading indicates regions higher than 1000 m above sea level. Rectangles outline the set of nested domains used for the evaluation of area-averaged precipitation in Section 4.2; the innermost is the D1 domain.

and amounts of rainfall in a heavy rainfall case. Souma et al. (2013) confirmed that both anthropogenic heat and artificial land cover increased the amount of precipitation in a localized heavy rainfall event in Tokyo. Inamura et al. (2011) modeled eight brief heavy rainfall events in Tokyo using five objective analysis datasets and concluded that urban effects altered the wind characteristics leeward of the urban area, developing wind convergence and rainfall there. Kusaka et al. (2014) examined the urban impact on the precipitation climatology of Tokyo using numerical simulations with four kinds of initial and boundary conditions and showed that urbanization resulted in a robust increase in the amount of precipitation in the Tokyo metropolitan area and a reduction in inland areas. Shimadera et al. (2015) showed that changes in land use from vegetation to urban resulted in a precipitation increase in the Osaka metropolitan area in western Japan.

In the present study, we conducted numerical experiments to extend our understanding of urban impacts on precipitation in Tokyo. Although previous studies have suggested that several urban characteristics can cause a precipitation response, the case studies mentioned above indicate that the urban effect does not necessarily enhance precipitation in Tokyo. In addition, the leading factor that modifies precipitation in urban

Table 1
Specifications of NHM in this study.

Governing equations	Fully compressible, non-hydrostatic
Discretization	Grid point method, z^* -coordinate
Treatment of advection	4th order flux form, advection corrected
Map projection	Lambert conformal projection
Topography	GTOPO30
Cloud microphysics	Bulk scheme with ice phase predicting qv , qc , qr , qi , qs , qg
Cumulus parameterization	Not used
Turbulent closure	Improved Mellor-Yamada level 3 (Nakanishi and Niino, 2006)
Cloud radiation	Kitagawa (2000)
Clear sky radiation	Yabu et al. (2005)
Clouds in radiation process	Partial condensation scheme
Surface flux	Beljaars and Holtslag (1991)
Urban canopy	SPUC scheme (Aoyagi and Seino, 2011)



areas is still unclear. Therefore, as a first step, we focused on thermodynamic forcing by an intensified heat island, because rising temperature is the most obvious feature of the city in recent decades. Comparative experiments were performed to investigate the influence, if any, of temperature change on monthly and daily precipitation. We mainly focus on August, the hottest month, in which influences of large-scale disturbance are relatively small and mesoscale convective activity is typically high. The numerical model and experimental design are described in the next section. Simulation results are presented in [Section 3](#) and discussed in [Section 4](#). Finally, conclusions are given in [Section 5](#).

2. Simulation method

2.1. Numerical model

This study used the Non-Hydrostatic Model (NHM) of the Japan Meteorological Agency (JMA), which has been an operational forecast model since 2004 ([Saito et al., 2006, 2007](#)). The NHM has also been used for a wide range of research, including tornadogenesis simulation and regional climate modeling ([Mashiko et al., 2009; Ishizaki et al., 2012; Saito, 2012](#)). We employed a horizontal grid interval of 2 km and a model domain covering central Japan ([Fig. 1a](#)). Convective parameterization was not used in view of the model resolution, and thus the moist convective process was dealt with directly in the cloud microphysics scheme. Other specifications of NHM in this study are summarized in [Table 1](#).

In highly built-up urban areas, canopy elements such as buildings increasingly affect the surface energy balance, and their effect should not be ignored. We employed the Square Prism Urban Canopy (SPUC) scheme ([Aoyagi and Seino, 2011](#)) to take this urban effect into account in land surface processes. The SPUC scheme is a single-layer urban canopy scheme ([Masson, 2000; Kusaka et al., 2001; Grimmond et al., 2010](#)) designed for evaluating heat, moisture, and radiation exchanges between the atmosphere and the surfaces of the ground, building walls, and roof. It assumes a regular array of box-shaped buildings (with square horizontal cross sections) in a model grid, instead of a two-dimensional (horizontally long) building geometry, for a better representation of urban morphology in Tokyo. Longwave and shortwave radiation in the urban canopy are estimated using a skyview factor and a time-varying sunlight factor, respectively. Precipitation trapping upon the canopy elements is also considered. The SPUC scheme is described in detail by [Aoyagi and Seino \(2011\)](#), with its validation results in the Kanto region.

2.2. Experimental design

We performed a series of comparative simulations for August of the eight years from 2006 to 2013, aiming to examine the impact of heat-island intensification on precipitation. In one set of experiments, the SPUC scheme was applied in highly urbanized grid cells in Tokyo and adjacent areas to represent the current urbanized condition (the CRNT experiment). In the other set of experiments, a slab land surface treatment was applied in the entire model domain, using urban surface parameters that represent moderately urbanized conditions (the MDUB experiment). The treatment of land surface processes was changed only in the grid cells in which SPUC was applied ([Fig. 1b](#)). In other areas, the experiments used the same land surface (slab) scheme and surface parameters. The same experiments were later conducted for the months of July and February (see [Section 4.2](#)).

The simulation was intended to examine precipitation modulations that are directly caused by slight temperature changes in the urban area. When precipitation differs between the CRNT and MDUB experiments, it naturally gives rise to differences in atmospheric environment and land surface conditions between the two experiments. To avoid the accumulation of such secondary influences, we repeated time integrations for each day of the month for 27 h starting at 2100 JST (Japan Standard Time; 0000 UTC = 0900 JST) of the previous day. Initial and boundary data were taken from operational mesoscale analyses of the JMA. Simulation results from forecast times FT = 3 to FT = 27 (from 0000 to 2400 JST) were used in the present analysis.

Fig. 2. Simulated surface air temperature in August averaged from 2006 to 2013 by (a) the CRNT experiment and (b) the MDUB experiment, and (c) the difference between the two experiments (CRNT – MDUB).

Grid-averaged land surface parameters (albedo, roughness length, thermal property, and initial wetness) were determined according to the area fractions of 11 land-use categories in each grid cell using the 100-m-mesh Digital National Land Information Dataset. Land surface parameters for each land-use category were similar to those usually used in NHM (Aoyagi et al., 2012; their Table 3) with a few exceptions. Thermal conductivity for the “building lot” land surface category was changed from 1.5×10^{-6} to $0.75 \times 10^{-6} \text{ m}^2 \text{ s}^{-1}$ to represent the moderately urbanized condition. The initial condition for wetness (evaporation efficiency) was modified from 0.02 to 0.06 for building lots to correct the underestimation of latent heat in urban areas noted by Aoyagi and Seino (2011).

In our simulations, the SPUC scheme was applied to highly urbanized grid cells where more than 80% of the grid area consists of artificial land uses (building lot, road, and other artificial surfaces). Use of the SPUC scheme was limited to Tokyo and surrounding urban areas (Fig. 1) for simplicity of analysis. Parameters representing urban canopy geometry in the SPUC scheme were determined as follows. Uniform building heights of 10 m and aspect ratios (ratio of height to width of buildings) of 0.5 were used to approximate actual building configurations in the area where SPUC was applied. Skyview and sunlight factors were evaluated from the building area fraction (Fig. 1) in each grid cell, assuming that buildings occupy 60% of the building lot area. Typical thermal properties for office building roofs and walls were used, as well as those given by Aoyagi et al. (2012; their Table 4). Time-dependent anthropogenic heat in the metropolitan area (Senoo et al., 2004) was considered in the cells where SPUC was applied. Although reduced wind speed in the canopy layer was taken into account in the heat flux formulation of the SPUC scheme, surface momentum flux was obtained in the same manner for both CRNT and MDUB experiments, using the same grid-averaged roughness length.

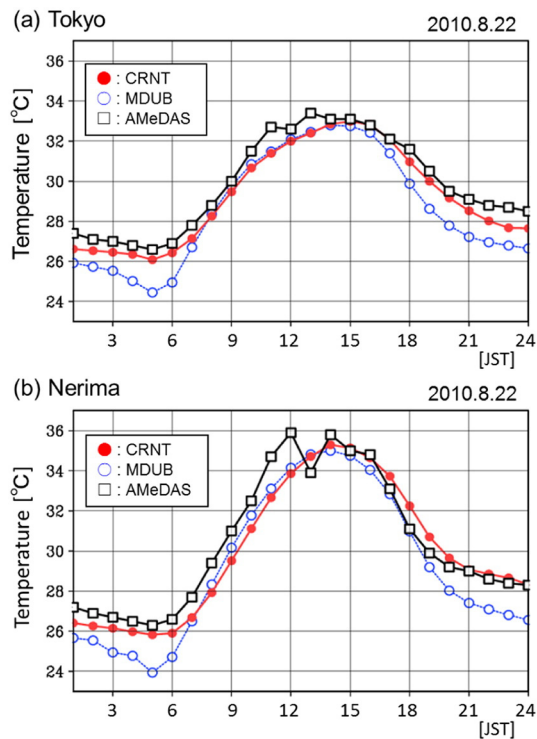


Fig. 3. Diurnal variations of simulated and observed surface air temperatures at (a) Tokyo and (b) Nerima on 22 August 2010. See Fig. 1b for station locations.

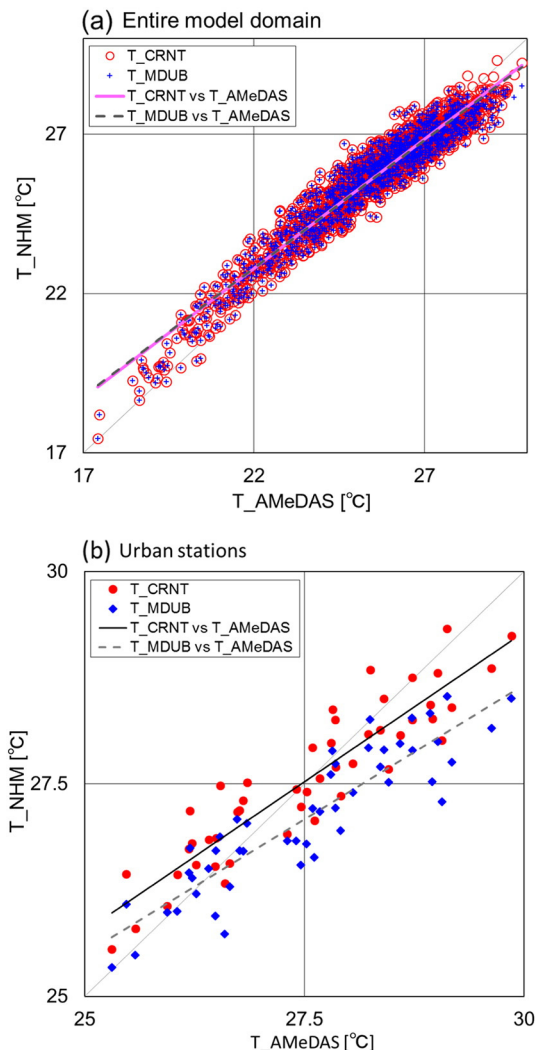


Fig. 4. Scatter plot of simulated versus observed monthly mean temperatures for August during 2006–2013 at stations (a) in the entire model domain and (b) in grid cells in which SPUC was applied.

Table 2
Validation of simulated monthly mean temperatures.

Domain/station	Number of data	Bias		Correlation coefficient	
		CRNT	MDUB	CRNT	MDUB
Entire model domain	1528	0.14	0.12	0.96	0.96
Kanto Plain	456	-0.11	-0.18	0.91	0.91
SPUC-applied area	48	0.02	-0.42	0.92	0.90
Tokyo	8	-0.36	-1.04	0.93	0.93
Nerima	8	0.04	-0.63	0.92	0.91

3. Results

3.1. Surface air temperature

We first examined the surface air temperature field using the hourly output of the simulation. Fig. 2 shows simulated monthly mean temperatures in the CRNT and MDUB experiments, averaged over Augusts of all eight years, and the difference between the experiments (CRNT – MDUB). On the average of the eight years, the simulated temperature in the CRNT experiment was 0.8 °C higher in the central urban area. Although the monthly mean temperature difference slightly varied from year to year, it was always positive in the cells where SPUC was applied in each year and was at most 1 °C in the central part of Tokyo.

Typical examples of the diurnal temperature variation on a sunny day at meteorological stations Tokyo (business district) and Nerima (residential district), both located in central Tokyo (see Fig. 1b), are shown in Fig. 3. Simulated temperatures in the CRNT experiment were higher than those in the MDUB experiment, except for the hours after sunrise, and generally agreed better with observations. The temperature difference between the experiments was associated with modifications of surface energy balance in response to the urban canopy geometry and anthropogenic heating (Aoyagi and Seino, 2011). Higher temperatures in the CRNT experiment in the afternoon and nighttime were caused by the release of sensible heat from the canopy elements that stored heat in the morning hours. These temperature variations between the two experiments demonstrate characteristic changes due to urbanization (Oke, 1987; Fujibe, 1997).

The simulated monthly mean temperatures were validated against AMeDAS observation data, using simulated temperatures at the land grid cell nearest to the AMeDAS station. When the elevation of the model grid cell differed by more than 75 m from the actual station elevation, the station was excluded from the validation to avoid the temperature bias due to elevation differences. Simulated temperatures were fairly well correlated with the observations in both experiments (Fig. 4). Although positive temperature biases (i.e., simulated temperatures higher than observations) appeared more frequently at lower temperatures, temperature differences between simulations and observations were within ± 1.0 °C in 88% and within ± 1.5 °C in 98% of the entire model domain. Differences in simulated temperatures between the CRNT and MDUB experiments were quite small except for the stations in the area where SPUC was applied. At those stations, negative biases found in the MDUB experiment were reduced in the CRNT experiment (Fig. 4b).

The mean bias and correlation coefficient of monthly mean temperature are summarized in Table 2 for the entire model domain, the Kanto Plain, the areas where SPUC was applied, and Tokyo and Nerima stations in the central urban area. Mean biases in the entire model domain and the Kanto Plain were acceptably small in both experiments. Simulated temperatures of the CRNT experiment were less biased in the cells where SPUC was applied. We can say that the CRNT experiment successfully simulated the current temperature field. The MDUB experiment, on the other hand, yielded slightly low temperatures in the urbanized area, indicating a smaller heat-island effect.

3.2. Monthly precipitation

Fig. 5 depicts observed monthly precipitation based on the JMA's Radar-rain gauge Analyzed Precipitation dataset. There are large year-to-year variations in the amount and spatial distribution of precipitation. The CRNT experiment simulated these variations reasonably well, except for areas along the lateral boundary (Fig. 6). After excluding the zone affected because of the boundary setting (as indicated in Fig. 6a), monthly precipitation amounts averaged over the inner domain were generally well simulated in both the CRNT and MDUB experiments (Fig. 7).

Fig. 8 shows the difference in monthly precipitation amounts between the CRNT and MDUB experiments. The differences were widely found, in contrast to the temperature difference, which was confined to the areas where SPUC was applied (see Fig. 2). Positive and negative precipitation anomalies frequently appeared close together, which suggests that slight changes in the location of precipitation occurred between the two experiments. The simulated precipitation distribution in the two experiments and their differences, averaged over the eight years of August data, are shown in Fig. 9. The urban influence can be seen more clearly in Fig. 9c than in Fig. 8. Positive precipitation anomalies were more common in the area where SPUC was applied, and

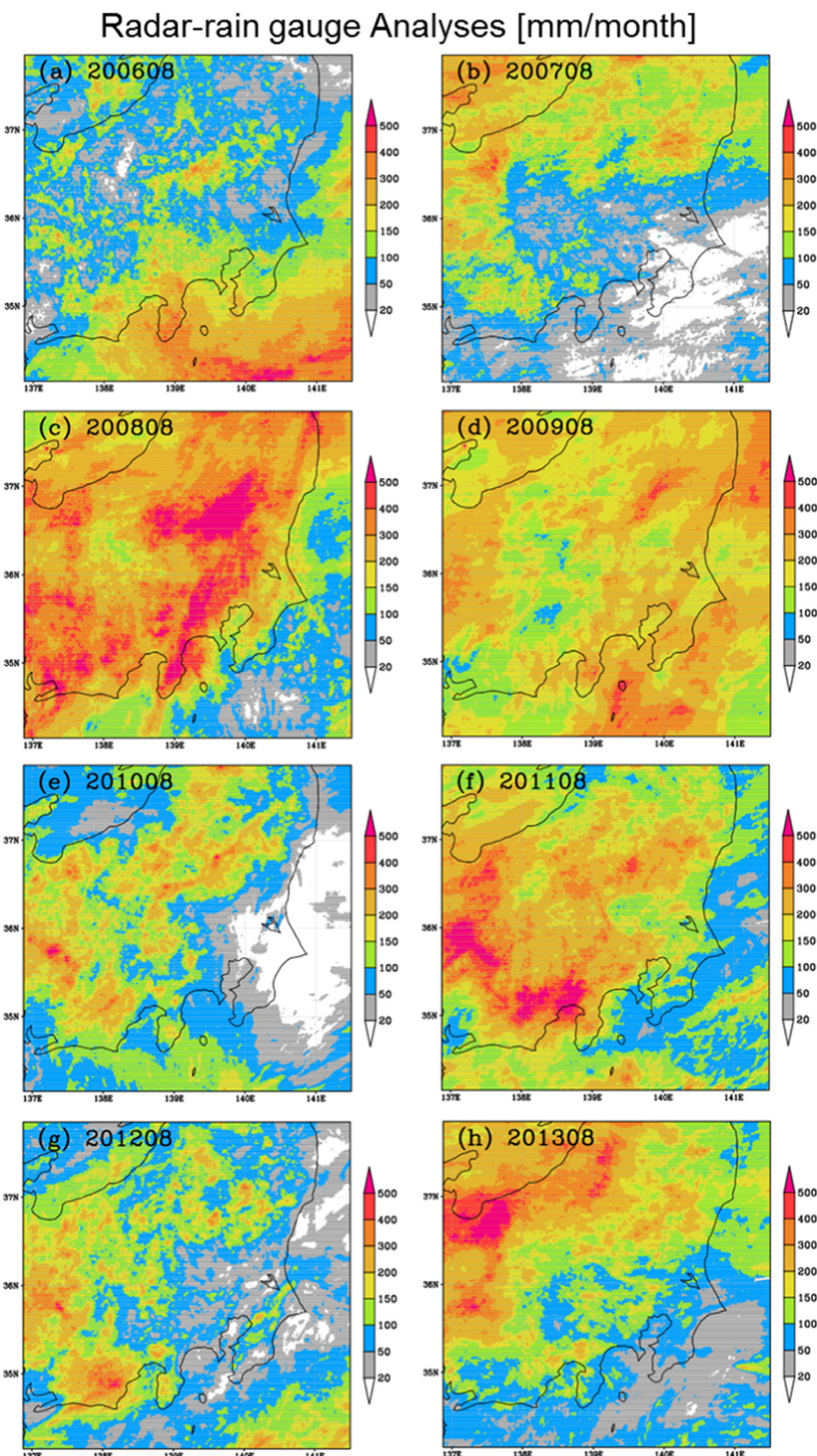
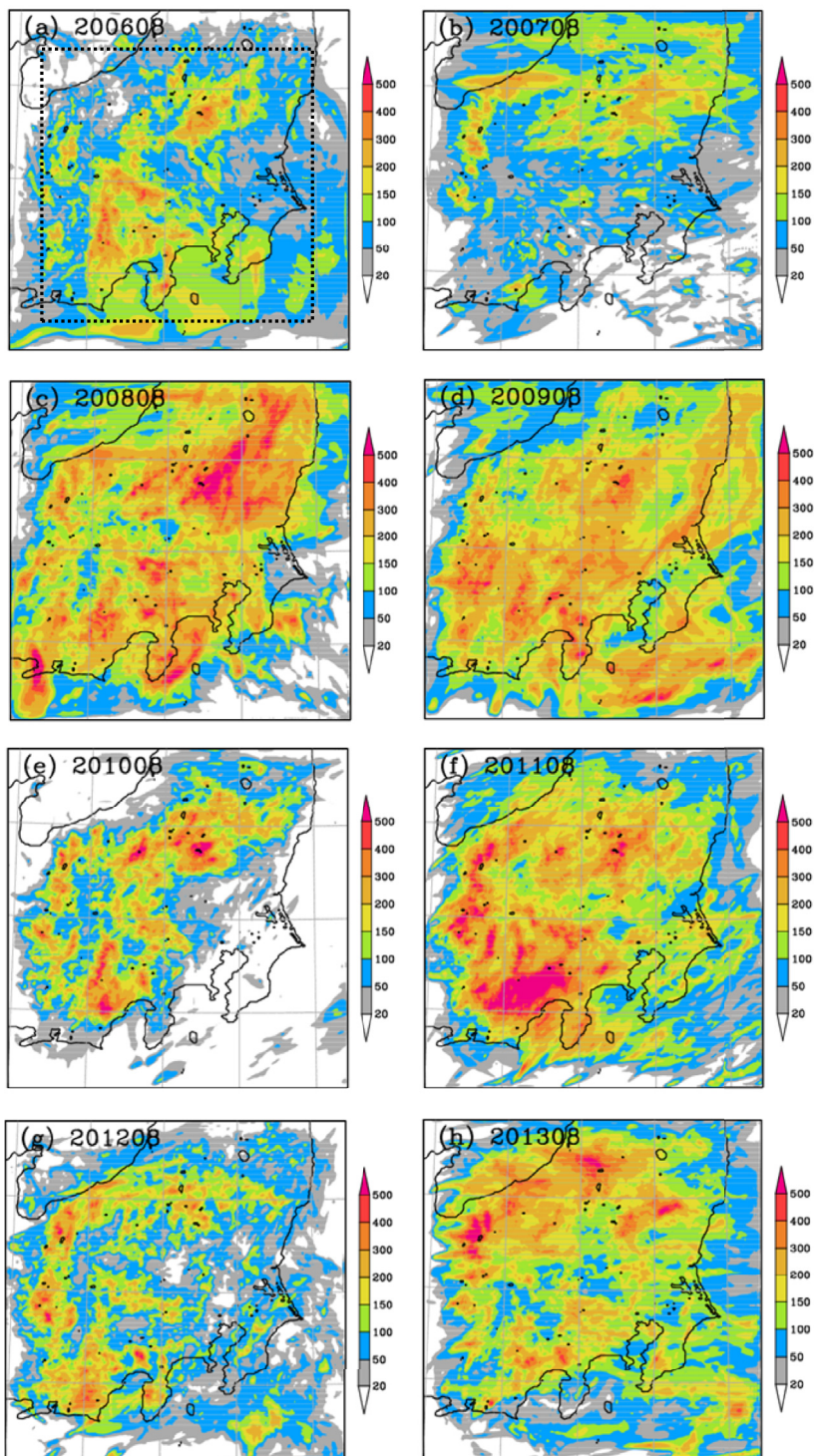


Fig. 5. Observed precipitation amounts in August of 2006 to 2013, obtained from JMA Radar-rain gauge Analyzed Precipitation data.

CRNT Monthly precipitation [mm/month]

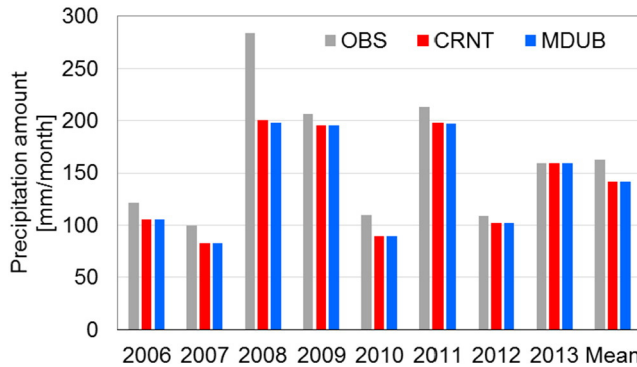


Fig. 7. Observed and modeled average monthly precipitation amounts for August of 2006 to 2013 for the domain outlined in Fig. 6a.

negative anomalies appeared north of this area in the inland part of the Kanto Plain. This precipitation modification pattern showed similarity to that of [Kusaka et al. \(2014\)](#).

Fig. 10 shows these anomalies in percentage terms. Positive anomalies were more apparent in highly urbanized areas, whereas negative precipitation anomalies in the northern part of the Kanto Plain were less clear because the mean precipitation amount there was slightly greater than near the coast (Fig. 9a and b). To smooth the spatial variability remained in Fig. 10, we considered area-averaged monthly precipitation (AMP) over 10 different sized domains (Fig. 1b) centered on the most highly urbanized area and having sides of length $(20k + 2)$ km ($k = 1\text{--}10$). Domain D4 covers most of the area where SPUC was applied and is referred to as the reference urban domain.

Fig. 11 illustrates the percent increase in AMP within these domains, defined as $(\text{AMP}_{\text{CRNT}} - \text{AMP}_{\text{MDUB}}) / \text{AMP}_{\text{MDUB}} \times 100$, for the mean of August in all eight years. Differences were positive for the six innermost domains, meaning that the CRNT experiment yielded larger values of AMP than the MDUB experiment in these domains. The difference was roughly 10% in the innermost domain D1 and grew smaller as the domain size increased. These differences were statistically significant by one-sided *t*-test at a significance level of 90% for domain D1 and 95% for domains D2–D6.

We also estimated AMP in the differential zones between adjacent domains (i.e., zone Z1 coincides with domain D1, zone Z2 denotes D2 – D1, etc.), shown as the broken line in Fig. 11. In each zone within D4, this “zonal difference” was positive. In outer zones, this difference was near or slightly below zero. Although zonal AMP values had relatively large deviations influenced by year-to-year changes in precipitation location, the zonal difference in AMP was statistically significant (at 90%) in zones Z1 to Z4. These results suggest that there was a substantial increase in monthly mean precipitation within the reference urban domain D4 in the CRNT experiment. In the outer areas between zones D4 and D9, the monthly precipitation amount was smaller in the CRNT experiment, which partially offset the precipitation increase within D4. Beyond domain D9, spatial deviations in precipitation were negligible relative to the domain average.

3.3. Daily precipitation

We further examined the modification of precipitation between the CRNT and MDUB experiments on a day-to-day basis. In the central urban domain D1, at least one experiment (CRNT or MDUB) simulated 1 mm or more daily precipitation in at least one grid cell on 105 of the 248 days (31 days in each of 8 years) of the simulation period. We compared the precipitation characteristics of the two experiments for these “rainy-day” cases. Fig. 12a is a scatter plot showing the numbers of grid cells in which simulated daily precipitation was 1 mm or more (Nr) in domain D1 for each of the 105 days. Fig. 12b is a similar plot showing the number of grid cells with heavy (≥ 20 mm/day) precipitation (Nh). Both Nr and Nh in domain D1 had a

Fig. 6. Simulated precipitation amount in August of 2006 to 2013 from the CRNT experiment. The outline in (a) shows the inner domain, which was chosen to avoid boundary effects and was used for the evaluation of domain-average precipitation shown in Fig. 7.

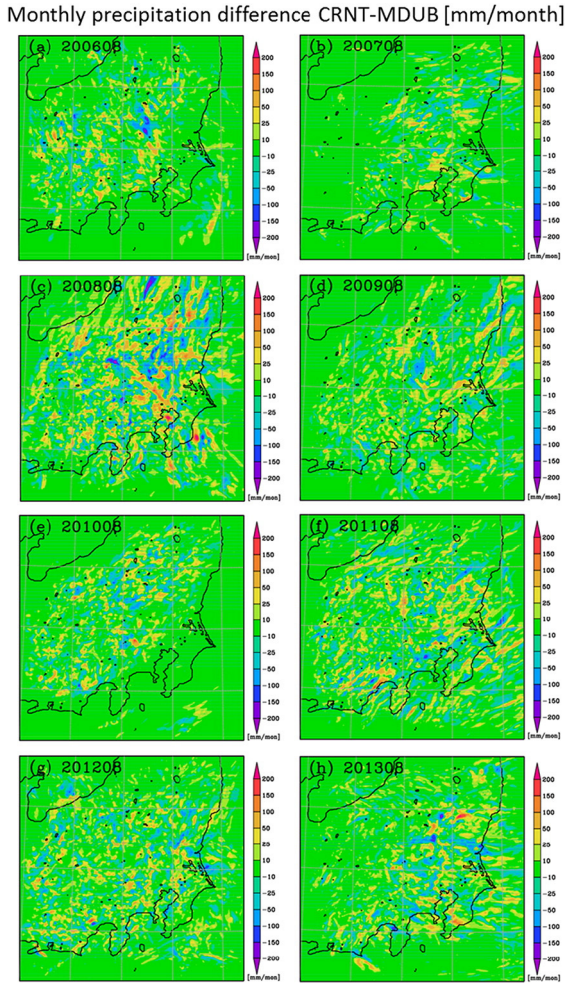


Fig. 8. Differences between monthly precipitation amounts simulated in the CRNT and MDUB experiments (CRNT – MDUB) for August from 2006 to 2013.

relatively large scatter between the CRNT and MDUB experiments, but regression lines with a slope very close to unity, which means that the spatial extent of precipitation was, on average, little biased by urban temperature change.

We also analyzed these rainy-day cases in terms of area-averaged daily precipitation (ADP), defined as the mean value of daily precipitation amounts over grid cells with precipitation in domain D1 (Fig. 12c), and area-maximum daily precipitation (MDP), defined as the maximum value of daily precipitation amounts among the grid cells in domain D1 (Fig. 12d). In both analyses, the slopes of the regression lines were slightly greater than 1, indicating larger values in the CRNT experiment (positive bias). Histograms of the differences in ADP and MDP (Fig. 13) show that positive deviations were more frequent than negative deviations.

Variations in Nr, Nh, and ADP between the two experiments became smaller and the mean bias in ADP gradually decreased in wider domains (figure not shown). However, biases in MDP persisted and varied as domain size increased (Fig. 14). In domains within D6, MDP biases were predominantly positive, as in D1. In domains larger than D8, negative biases increasingly appeared. In domain D10 and over the whole model domain, positive and negative biases appeared almost equally often.

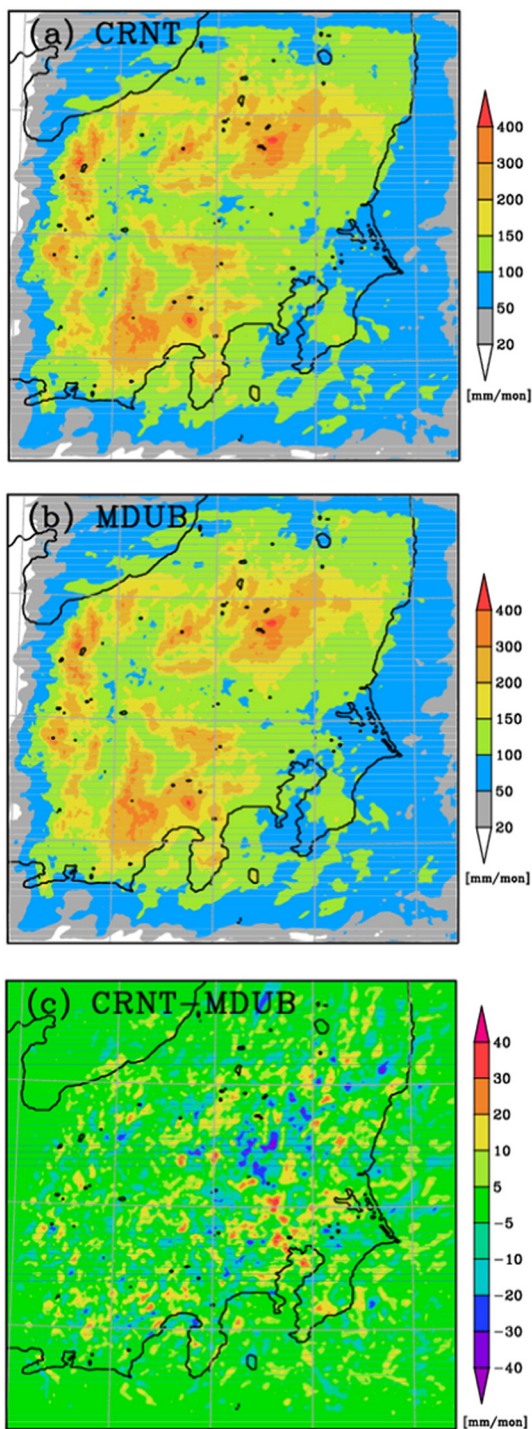


Fig. 9. Simulated monthly precipitation amounts averaged over all Augests from 2006 to 2013 in (a) the CRNT experiment and (b) the MDUB experiment, and (c) the difference between these results (CRNT – MDUB).

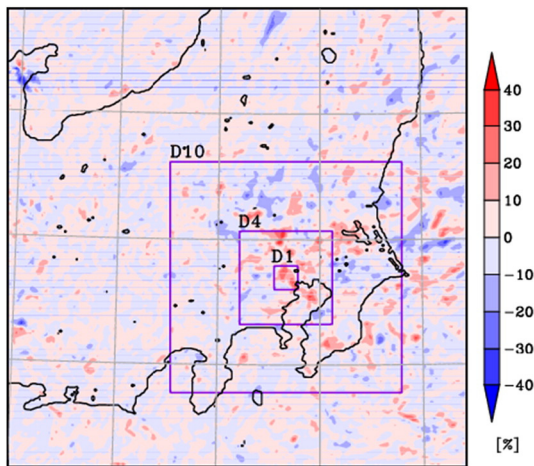


Fig. 10. Normalized precipitation difference with reference to the MDUB precipitation amount (percent rate) for all Augests of 2006–2013.

4. Discussion

4.1. Processes relevant to precipitation change

The CRNT experiment simulated higher surface air temperatures in the Tokyo area (see Section 3.1). In this section, we discuss how that temperature difference and related processes may have contributed to the precipitation differences between the CRNT and MDUB experiments.

At mesoscale, the winds and temperatures around Tokyo are generally affected by the sea-breeze circulation (e.g., Yoshikado, 1992). Carter et al. (2012) confirmed that the urban environment can have an impact on

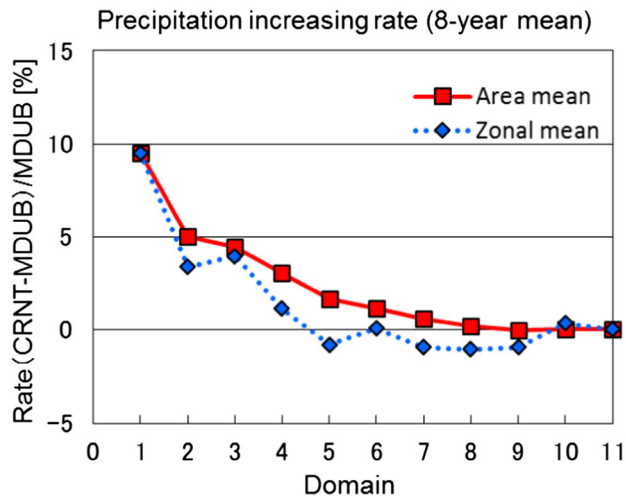


Fig. 11. Eight-year mean changes in area-averaged monthly precipitation in domains D1–D10 and the entire model domain (domain 11). The solid red line indicates the domain average, and the dotted blue line indicates the average in the differential areas between domains (the areas not shared with smaller domains).

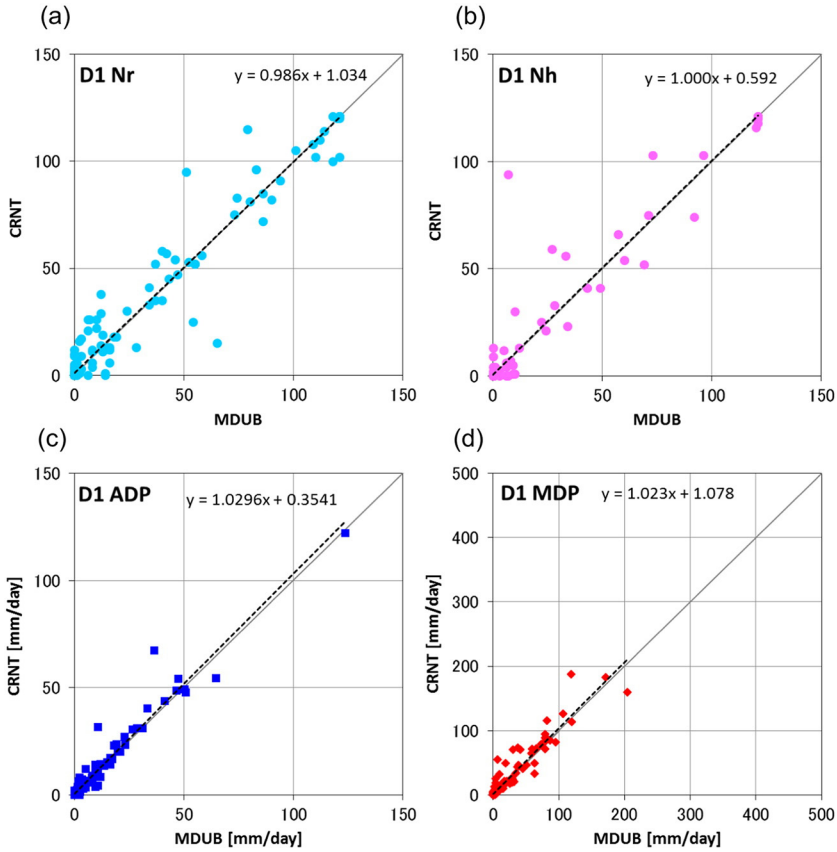


Fig. 12. Scatter diagrams between the daily CRNT and MDUB simulation results in (a) number of grid cells with simulated precipitation (Nr), (b) number of grid cells with heavy ($>= 20 \text{ mm/day}$) precipitation (Nh), (c) area-averaged daily precipitation amount (ADP), and (d) area-maximum daily precipitation amount (MDP) in domain D1.

the evolution of the sea-breeze mesoscale boundary, in their simulation using the Advanced Research Weather Research and Forecasting model (ARW-WRF) coupled to an atmosphere–land surface–urban canopy model. Our CRNT model results satisfactorily reproduced the development of the sea breeze and associated diurnal variations in wind and temperature. Fig. 15 depicts a composite field of surface wind (at roughly 20 m above ground level) and surface air temperature (at 1.5 m above ground level) over the course of the day for “no rain” cases (67 out of 248 days), in which simulated daily precipitation within the reference urban domain D4 was less than 1 mm or absent in both experiments. In the morning hours, surface winds are weak and onshore flow is not yet apparent (Fig. 15a, b). By noon, the sea breeze appears and begins to move inland (Fig. 15c). At 1500 JST, the sea breeze advances further and several wind shear zones form between inflows that originate from different coastal areas (Fig. 15d). An increase in temperatures can be seen during these hours. As the sea breeze continues, the area of highest temperature moves inland in the afternoon (Fig. 15e). By 2100 JST, the sea breeze ceases but temperatures remain high in the coastal area (Fig. 15f).

Differences in the surface air temperature between the CRNT and MDUB experiments (ΔT_s) are shown in Fig. 16. In the early morning, positive ΔT_s values appear in the central urban area associated with a pronounced heat island (Fig. 16a). At 0900 and 1200 JST, negative ΔT_s values, opposite to the daily mean difference (Fig. 2c), are found in the central urban area because the temperature rise is slow in the morning hours in the grid cells where SPUC was applied (Fig. 16b, c). By 1500 JST, ΔT_s turns positive (Fig. 16d). The temperature

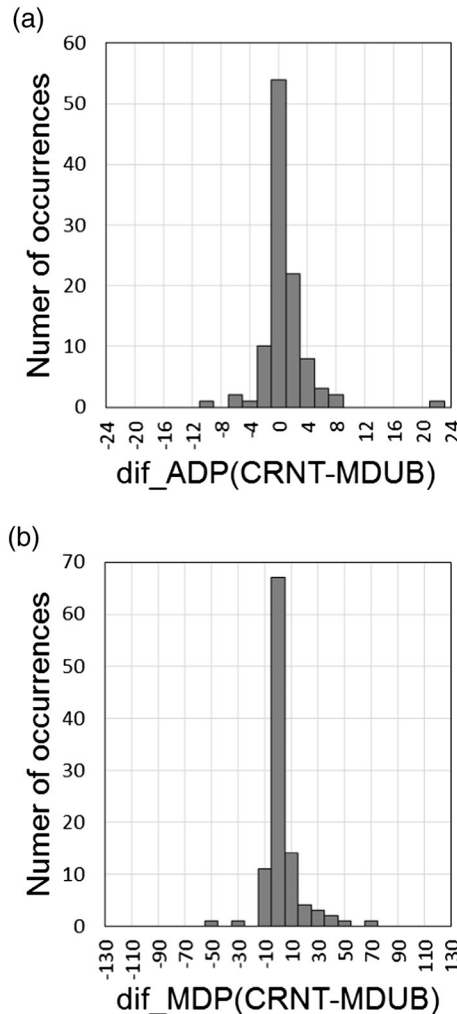


Fig. 13. Histogram of the daily differences in (a) ADP and (b) MDP between the CRNT and MDUB experiments in domain D1.

anomaly increases in the evening hours (Fig. 16e, f) and remains at that magnitude until the next sunrise, as shown in Fig. 3.

The difference in surface winds between the experiments was closely related to ΔT_s . Here, the composite of wind difference ($\Delta U, \Delta V$) is defined as $(U_{CRNT} - U_{MDUB}, V_{CRNT} - V_{MDUB})$ using the vector average wind of each experiment. Negative temperature anomalies are accompanied by outgoing flow from the area, and positive temperature anomalies appear with inflow to the area. Comparison of Fig. 16c and Fig. 15c indicates that in the CRNT experiment, the onshore wind component was weakened and the sea breeze advance was retarded at 1200 JST over the central urban area. At 1500 JST, inflow to the high-temperature anomaly slightly northwest of the central urban area became apparent. A similar differential circulation was found over the central urban area at 2100 JST (Fig. 16g, h). Figs. 15 and 16 show that the urban impact on surface temperature and associated thermally-induced flow had a clear diurnal variation in addition to the sea-breeze circulation and that complex time-varying urban-sea breeze interaction existed, as investigated in Carter et al. (2012).

In the rainy-day cases, surface winds and temperatures were disturbed by precipitation and become more complicated, but the discrepancies of the surface field between the CRNT and MDUB experiments generally resembled those in the no-rain cases. To more closely examine how the basic state of rainfall onset was modified, we selected 68 cases in which afternoon precipitation was simulated in domain D1 without precipitation

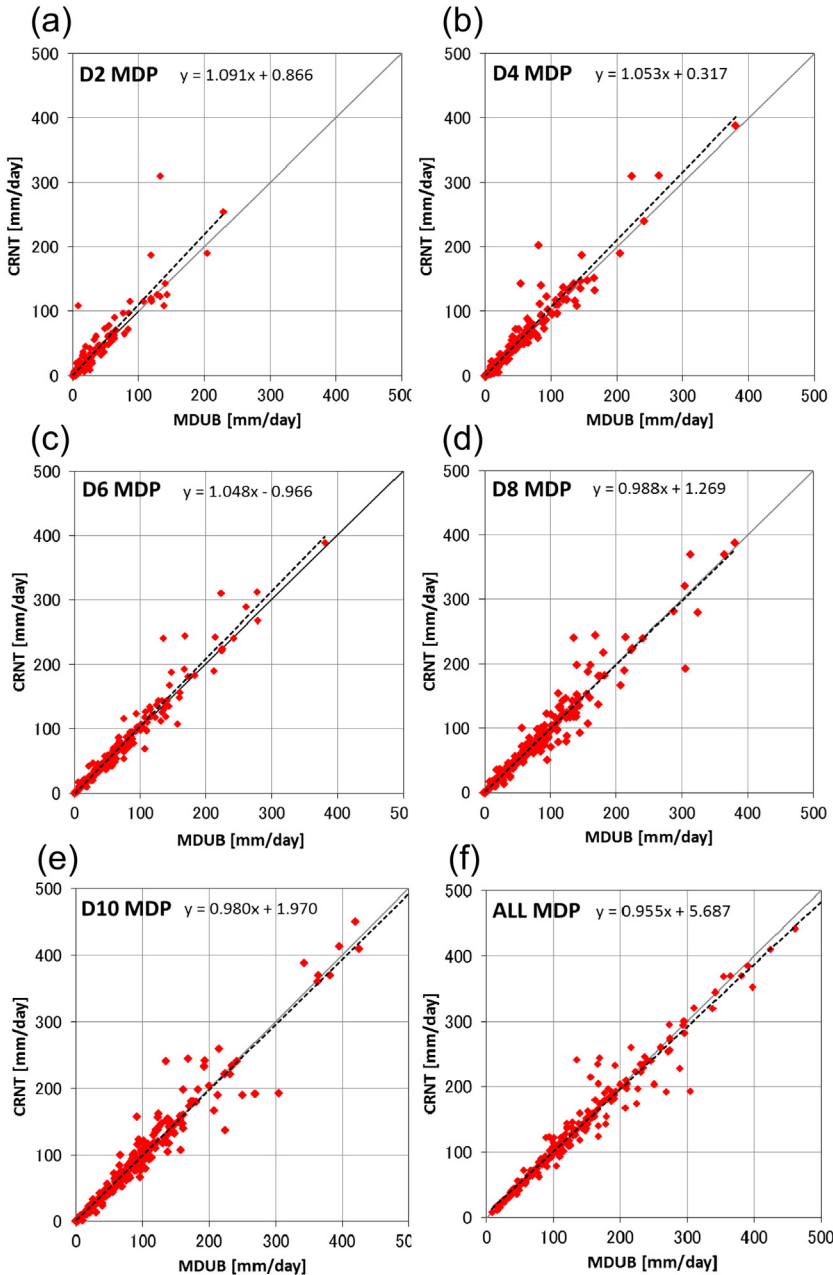


Fig. 14. Scatter diagrams between the daily CRNT and MDUB simulation results for MDP in domains D2, D4, D6, D8, D10, and the entire model domain.

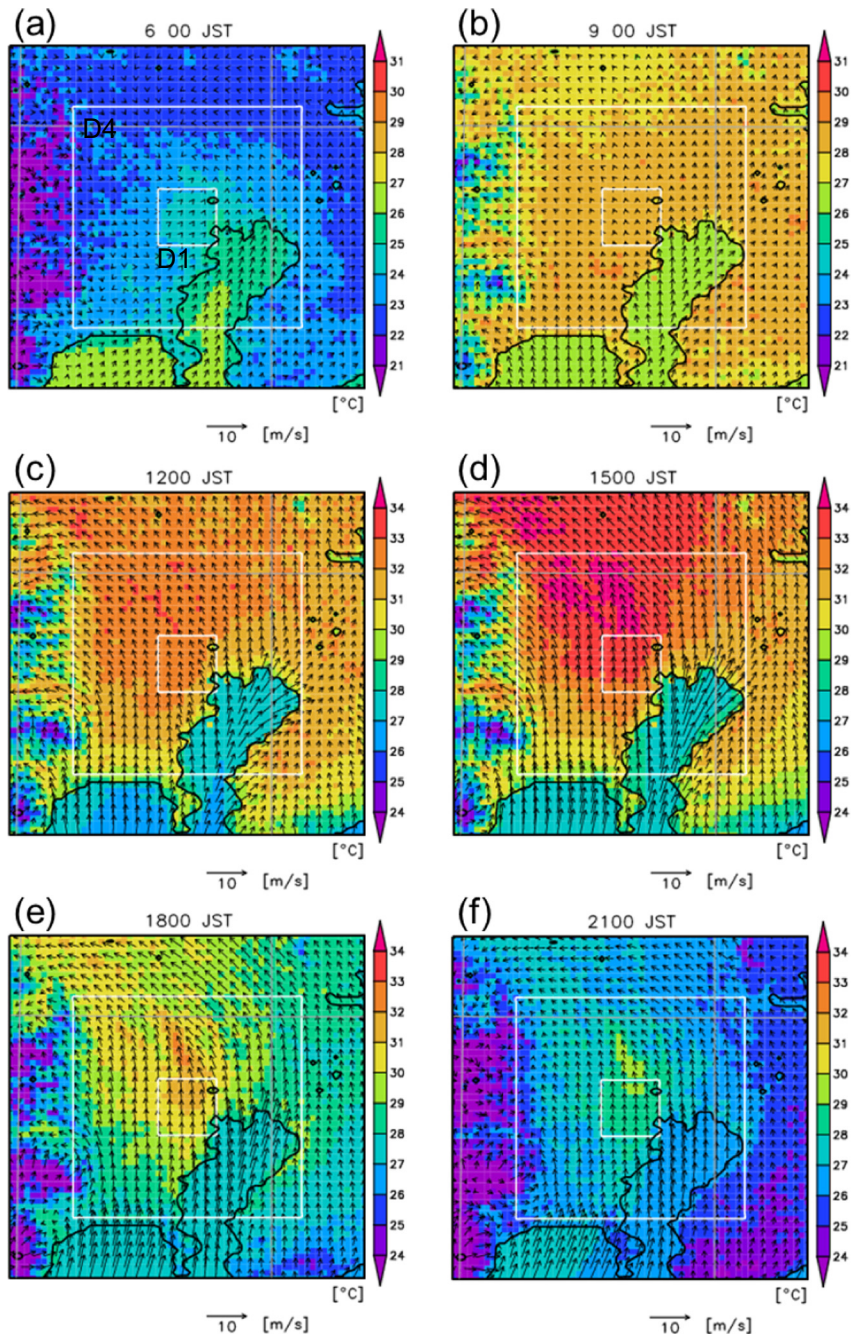


Fig. 15. Composite map of domain D6 showing the average surface winds and temperatures simulated in the CRNT experiment at 3-hour intervals starting at 0600 JST for no-rain cases in domain D4 (large rectangle).

in the preceding six hours (referred to as D1-NPP cases). We chose these cases because urban-induced precipitation is most likely to develop in this setting during the warm season (Fujibe et al., 2009) and because the mean precipitation increase in the CRNT experiment was most marked in domain D1, as mentioned in

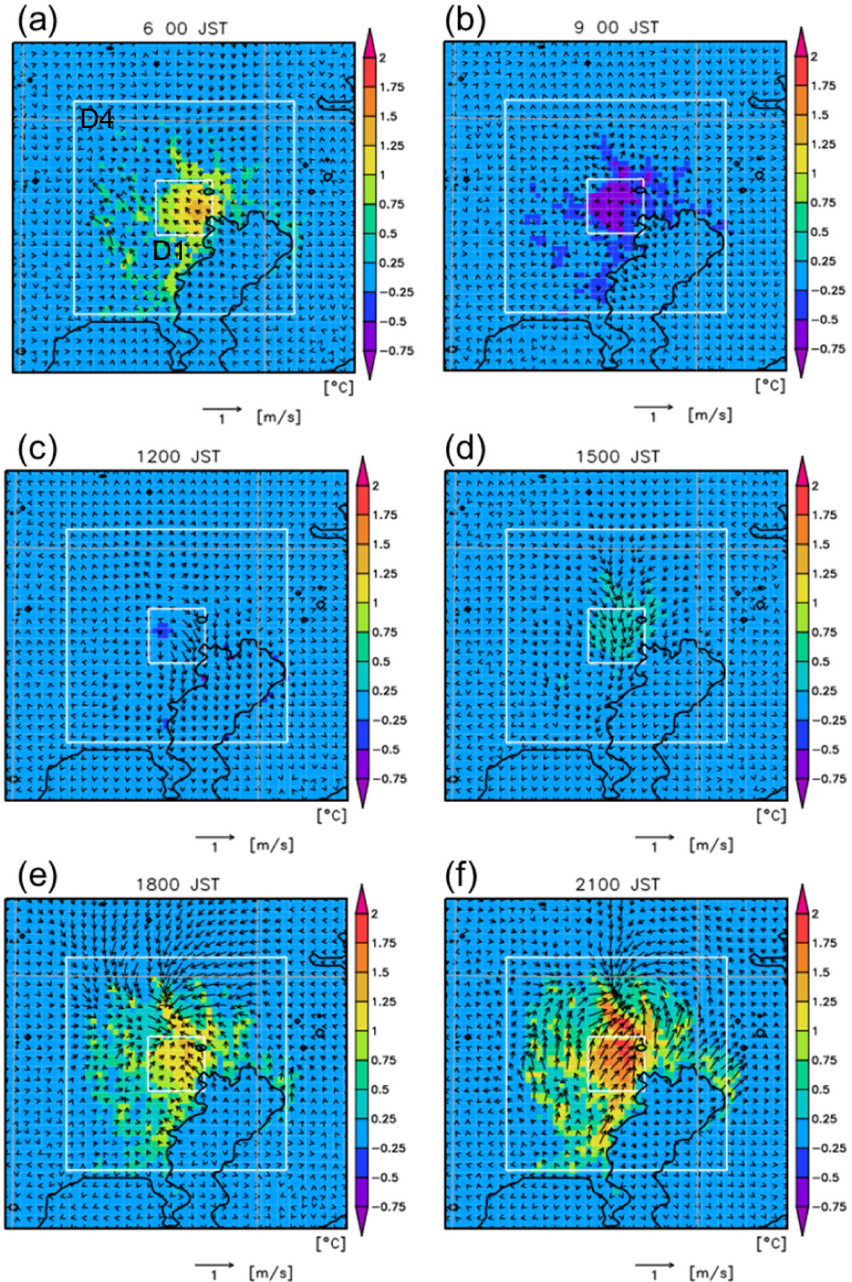


Fig. 16. Composite map of domain D6 showing the differences in surface winds and temperatures between the CRNT and MDUB experiments at 3-hour intervals starting at 0600 JST for no-rain cases in domain D4.

Section 3.2. As Fig. 17 shows, the precipitation increase in the CRNT experiment tended to appear around domain D1 in the D1-NPP cases, as well as the monthly mean precipitation difference shown in Fig. 9c. However, outside domain D4, the spatial pattern of the precipitation difference changed from the pattern shown in Fig. 9c.

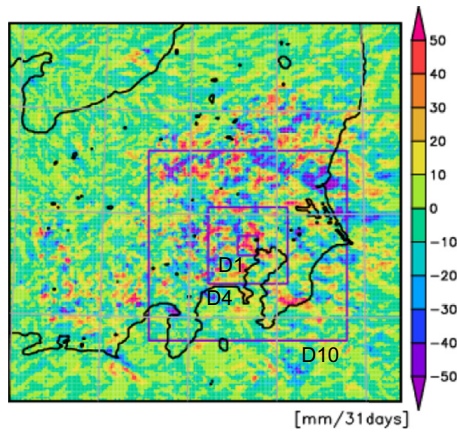


Fig. 17. Average precipitation differences between the CRNT and MDUB experiments in D1-NPP cases. Precipitation amounts are extrapolated to 31 days for comparison with monthly averages shown in Fig. 9c.

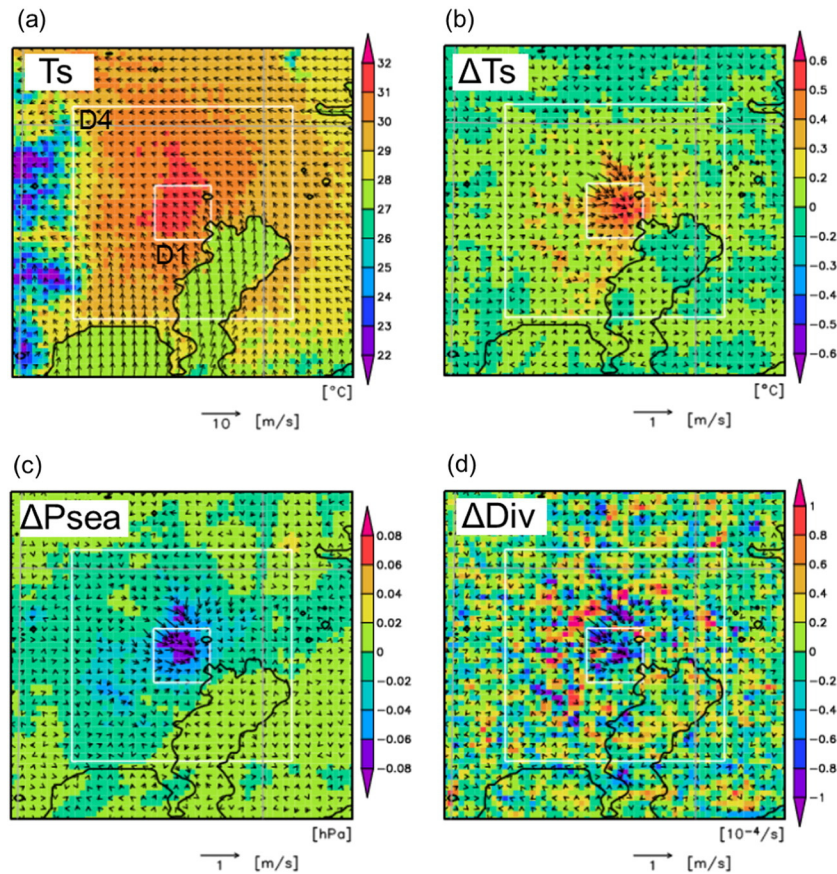


Fig. 18. Composite map of D1-NPP cases at 1 h before the onset of precipitation for (a) surface wind and temperature of the CRNT experiment, and differences in (b) surface wind and temperature, (c) sea-level pressure, and (d) surface divergence between the CRNT and MDUB experiments.

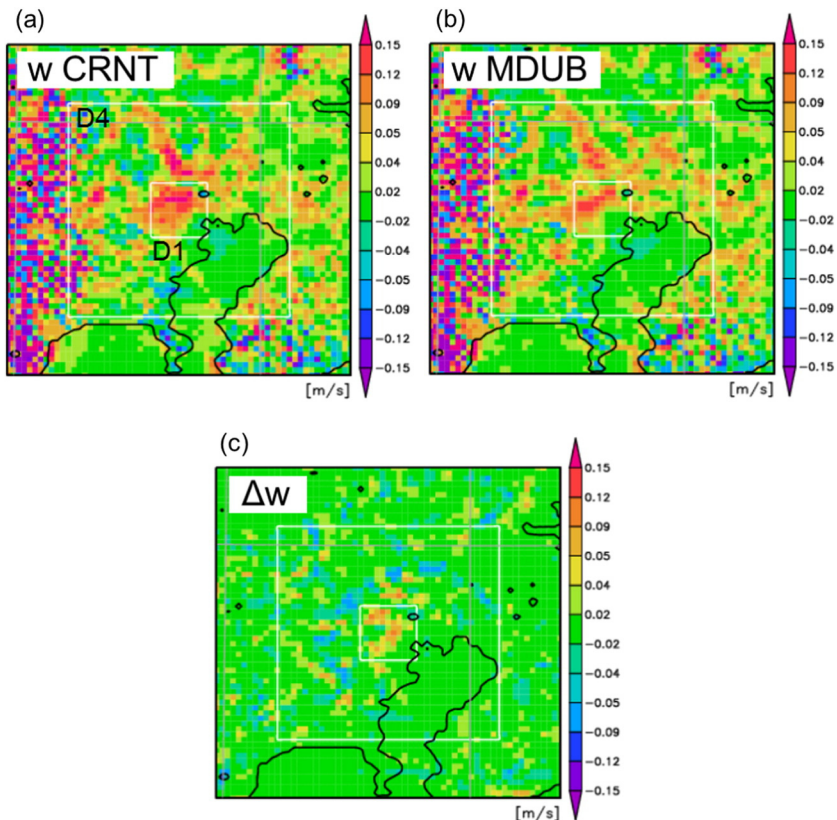


Fig. 19. Composite map of D1-NPP cases at 1 h before the onset of precipitation for vertical velocity at 936 m above sea level in (a) the CRNT experiment and the (b) MDUB experiment, and (c) their difference.

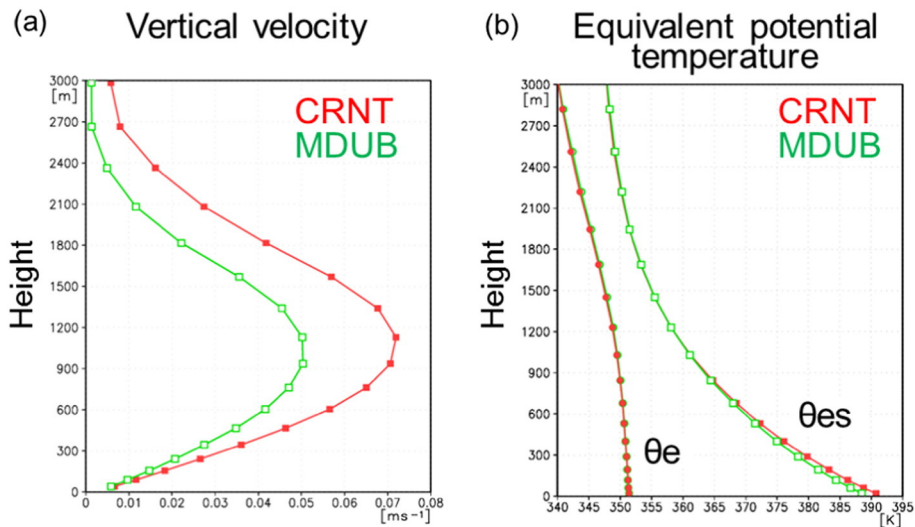
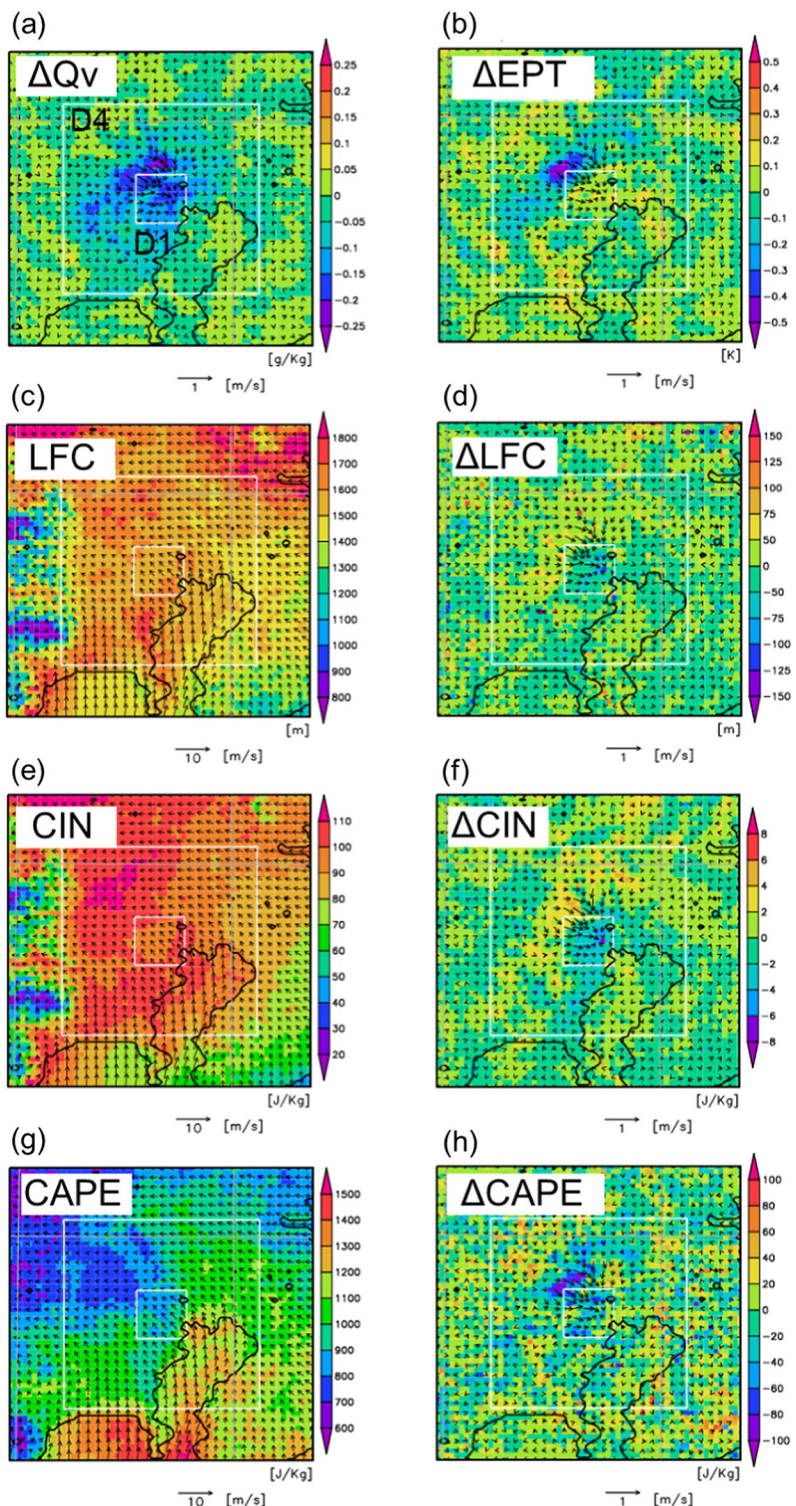


Fig. 20. Vertical profiles of (a) vertical velocity and (b) equivalent potential temperature (θ_e) and saturated equivalent potential temperature (θ_{es}) in the CRNT and MDUB experiments.



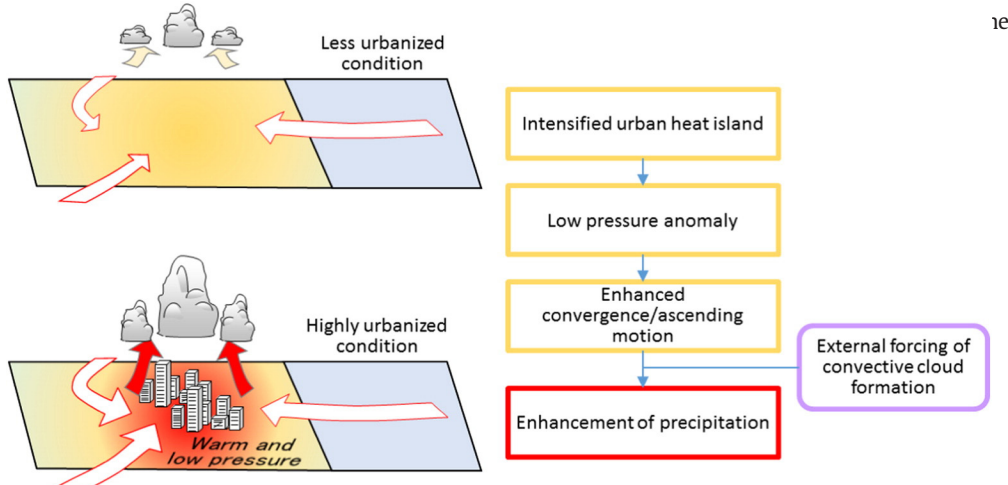


Fig. 22. Schematic illustration of the impact of urban temperature rise on precipitation and relevant processes. The upper panel shows less urbanized condition in the MDUB experiment. The lower panel shows highly urbanized condition in the CRNT experiment.

mean time of the composite is about 1530 JST, and thus the composite field is similar to that at 1500 JST in the no-rain cases. The warmest area in the composite CRNT field is located in and north of domain D1 (Fig. 18a). The composite differential map (Fig. 18b) shows that the surface air temperature in the CRNT experiment was 0.5 °C higher in domain D1, and a decrease in sea-level pressure associated with low-level temperature rise can also be seen around D1 (Fig. 18c). The surface-wind difference plot (Fig. 18d) clearly shows inflow to this area and intensified convergence (negative divergence) in the CRNT experiment.

These changes indicate that heat-island circulation in the CRNT experiment was, on average, enhanced around domain D1 before the onset of precipitation. The resulting intensification of horizontal convergence, promoting the formation and enhancement of convection, can reasonably explain the simulated increase in precipitation amount in the central urban domain. Changes in circulation were not limited to the surface level: ascending motion was roughly 40% stronger in the CRNT experiment than in the MDUB experiment in domain D1, as shown in the composite map at about 900 m above sea level (Fig. 19) and in area-average vertical profiles of vertical velocity (Fig. 20).

The surface vapor mixing ratio in domain D1 decreased slightly (less than 2%) in the CRNT experiment, and thus the increase in equivalent potential temperature associated with the modeled temperature rise was somewhat suppressed (Fig. 21). The decreased vapor amount in the CRNT experiment is explained by reduced surface evaporation in the building lots as a result of the partial replacement of ground surface by building roofs and walls with no evaporation, although anthropogenic latent heat partly offsets this reduction. In contrast to the vertical velocity, the distinction between the two experiments is very small in profiles of equivalent potential temperature and saturated equivalent potential temperature (Fig. 20b). Consequently, changes between the experiments in the stability indices of moist convection were limited: The levels of free convection (LFC; Fig. 21d) and the convective inhibition (CIN; Fig. 21f) decreased in the CRNT experiment, which is favorable for the initiation of moist convection. However, these changes were less than 5% in much of domain D1. Another widely used index, the convective available potential energy (CAPE), which indicates the potential for convective cloud development, even decreased around domain D1 (Fig. 21h).

Fig. 21. Composite map of D1-NPP cases at one hour before the onset of precipitation for (a) differences in vapor mixing ratio Q_v, (b) differences in equivalent potential temperature EPT, (c) level of free convection LFC, (d) differences in LFC, (e) level of convective inhibition CIN, (f) differences in CIN, (g) convective available potential energy CAPE, and (h) differences in CAPE.

Qualitatively similar contrasts between the two experiments are seen in ascending motion, vapor mixing ratio, and stability indices in the 1500 JST composite of no-rain cases (figure not shown). These results suggest that enhanced heat-island circulation, particularly enhanced ascending motion at around the central urban domain, can largely account for precipitation increases in the CRNT experiment, as schematically shown in Fig. 22.

4.2. Simulations for July and February

We carried out additional simulations for July (2006–2013) and February (2007–2014) to assess the seasonal variation of the urban impact on precipitation. The simulated mean surface air temperature difference was 0.7 °C in July, slightly smaller than in August, and 1.3 °C in February, larger than in August, in the central urban domain. As was the case for August, eight-year averaged monthly simulated precipitation amounts in July and February agreed reasonably well with observations (Fig. 23). An increase in precipitation in domain D4 was found for July, although it was slightly reduced compared with the August case (Fig. 24a). The precipitation increase for February was less than 5% and was limited to narrower areas (Fig. 24b).

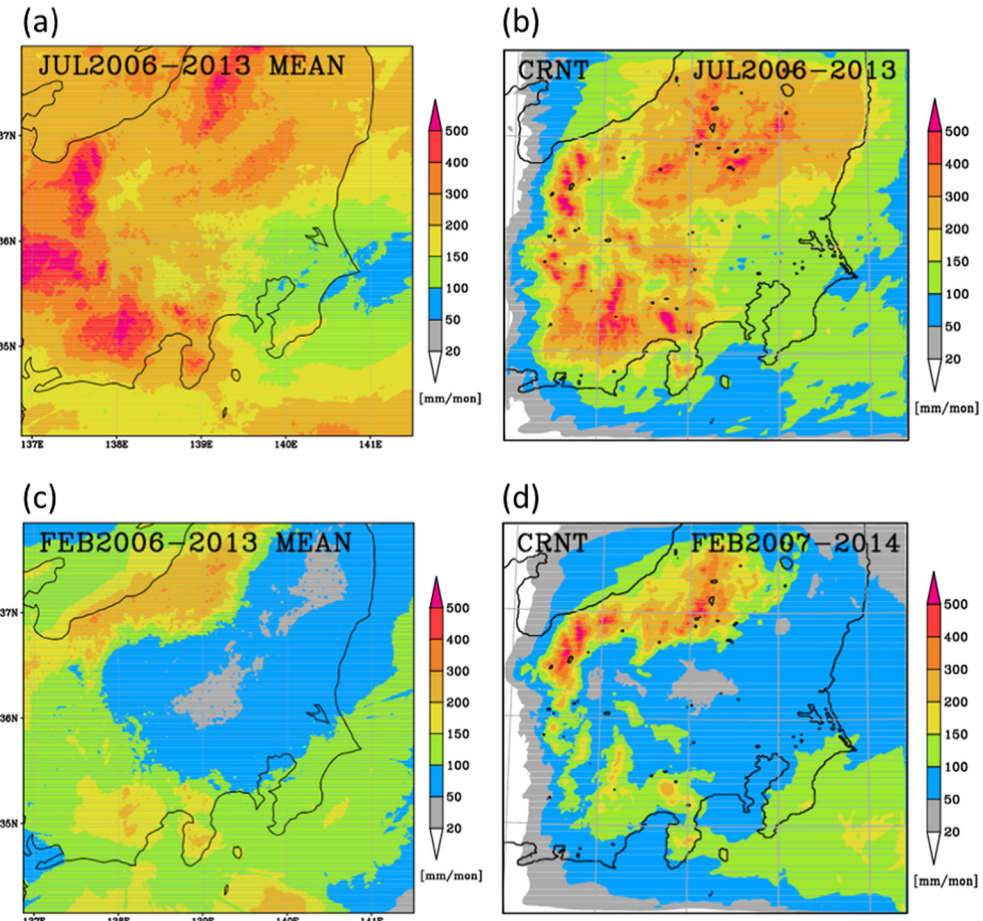


Fig. 23. Observed and simulated (CRNT) monthly precipitation amounts in July and February of eight years.

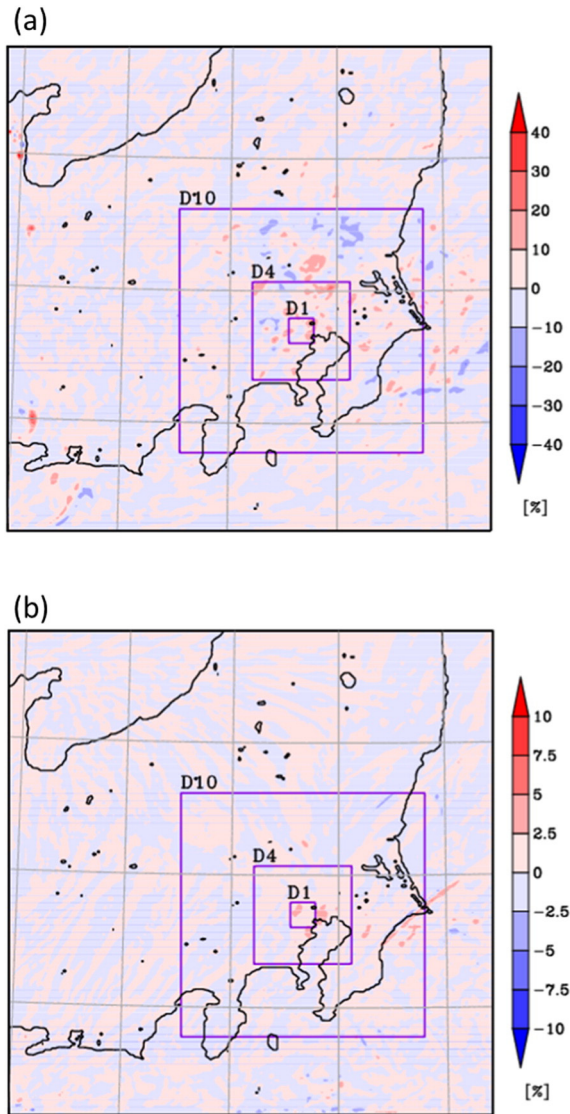


Fig. 24. Same as in Fig. 10, but for (a) July 2006–2013 and (b) February 2007–2014. Note that the range of color shades in Fig. 24(b) differs from that in Fig. 24(a).

The simulated seasonal contrast in precipitation modification can be explained by the seasonal variation in frequency of convective cloud formation (higher frequency in summer and less in winter) and synoptic-scale disturbance activity (more frequent in winter) in this region. Fujibe et al. (2009) showed that the influence of urbanization on precipitation in Tokyo is most clearly detected in the afternoon in summer and is less clear in other seasons. As discussed in Sections 4.1 and 4.2, our simulation results are consistent with their result and suggest that the pronounced urban heat island around Tokyo can have a detectable impact on precipitation in the warm season by enhancing dynamic processes in convective cloud development.

5. Conclusions

We investigated the impact of urbanization on precipitation in Tokyo and surrounding areas. A series of daily simulations was conducted using the NHM with the current highly urbanized (CRNT) condition and a moderately urbanized (MDUB) condition for the summer season (August and July) in the years 2006–2013 and February in the years 2007–2014.

The simulation results suggest that a mean temperature rise of less than 1 °C in Tokyo can lead to a statistically significant increase in August precipitation amount in the roughly 60 km square domain surrounding Tokyo. The increase reached 10% in the most urbanized (22 km square) domain. A similar increase was simulated for July, but no clear precipitation increase was simulated for February probably because of less convective activity. The simulated precipitation increase in the central urban domain was in agreement with the results of Kusaka et al. (2014), whose modeling considered the land-use change from grassland to urbanized conditions. In addition, the seasonal variation in the urban impact revealed in the present simulation agrees reasonably well with the findings of Fujibe et al. (2009). The thermal impact of urbanization in our simulation is likely an essential factor in the changes in precipitation in Tokyo.

We also examined the modification of daily precipitation characteristics in the two experiments. Both area-averaged and area-maximum daily precipitation amounts tended to be larger in the urbanized domain. Our simulation results indicate that the urban impact on the amount and spatial distribution of daily precipitation varied widely, which is consistent with the diversity of precipitation responses to urbanization found in previous case studies in Tokyo (Matheson and Ashie, 2008; Shimoju et al., 2010; Inamura et al., 2011). Composite analyses for periods before the onset of rainfall on rainy days further showed that thermally induced changes in circulation, rather than changes in static stability, played an important role in the simulated precipitation increase in the Tokyo urban area.

The settings of our comparative experiment were rather simplified, and thus the contrast in urban surface conditions between the CRNT and MDUB experiments does not exactly correspond to actual secular changes that have occurred in Tokyo. However, nearly 1 °C temperature rise simulated in this study is close to the summertime mean temperature increase ascribed to urbanization in the last 100 years at Tokyo (JMA, 2015), deduced from a comparison with the mean temperature rise in 15 rural stations. It should be noted that the precipitation increase in this study was simulated without an increase in the vapor amount in the monthly mean field or in the composite prior to the onset of rainfall.

Our simulation showed a wide variety of precipitation changes in individual daily cases, some of which are not fully explained by the processes apparent in the composite field. However, further detailed consideration is beyond the scope of the present study. For better understanding of precipitation modifications due to urbanization, the relative importance of other possible factors should be investigated in future studies.

Acknowledgments

We thank Drs. Teruyuki Kato, Wataru Mashiko, Hiromu Seko, Fumiaki Fujibe, and an anonymous reviewer for their helpful comments and suggestions. This work is partly supported by the SOUSEI program of the Ministry of Education, Culture, Sports, Science, and Technology (MEXT) of Japan.

References

- Aoyagi, T., Seino, N., 2011. A square prism urban canopy scheme for the NHM and its evaluation on summer conditions in the Tokyo metropolitan area, Japan. *J. Appl. Meteorol. Climatol.* 50, 1476–1496.
- Aoyagi, T., Kayaba, N., Seino, N., 2012. Numerical simulation of the surface air temperature change caused by increases of urban area, anthropogenic heat, and building aspect ratio in the Kanto-Koshin area. *J. Meteor. Soc. Japan* 90B, 11–31.
- Ashley, W.S., Bentley, M.L., Stallins, J.A., 2012. Urban-induced thunderstorm modification in the Southeast United States. *Clim. Chang.* 113:481–498. <http://dx.doi.org/10.1007/s10584-011-0324-1>.
- Baik, J.J., Kim, Y.-H., Chun, H.-Y., 2001. Dry and moist convection forced by an urban heat island. *J. Appl. Meteorol.* 40, 1462–1475.
- Balling, R.C., Brazel, S.W., 1987. Recent changes in Phoenix, Arizona summertime diurnal precipitation patterns. *Theor. Appl. Climatol.* 38: 50–54. <http://dx.doi.org/10.1007/BF00866253>.
- Beljaars, A.C.M., Holtslag, A.A.M., 1991. Flux parameterization over land surfaces for atmospheric models. *J. Appl. Meteorol.* 30, 327–341.
- Bornstein, R., Lin, Q., 2000. Urban heat islands and summertime convective thunderstorms in Atlanta: three case studies. *Atmos. Environ.* 34:507–516. [http://dx.doi.org/10.1016/S1352-2310\(99\)00374-X](http://dx.doi.org/10.1016/S1352-2310(99)00374-X).

- Carter, M., Marshall Shepherd, J., Burian, S., Jeyachandran, I., 2012. Integration of lidar data into a coupled mesoscale-land surface model: a theoretical assessment of sensitivity of urban-coastal mesoscale circulations to urban canopy parameters. *J. Atmos. Ocean. Technol.* 29:328–346. <http://dx.doi.org/10.1175/2011JTECHA1524.1>.
- Changnon Jr., S.A., 1981. METROMEX: A Review and Summary. *Meteor. Monogr.* 40. Amer. Meteor. Soc. (181 pp).
- Changnon, S.A., 2001. Assessment of historical thunderstorm data for urban effects: the Chicago case. *Clim. Chang.* 49, 161–169.
- Changnon Jr., S.A., Semonin, R.C., Huff, F.A., 1976. A hypothesis for urban rainfall anomalies. *J. Appl. Meteorol.* 15, 544–560.
- Dixon, P.G., Mote, T.L., 2003. Patterns and causes of Atlanta's urban heat island-initiated precipitation. *J. Appl. Meteorol.* 42, 1273–1284.
- Fujibe, F., 1997. Time-of-the-day dependence of long-term temperature changes at urban meteorological stations in Japan. *J. Meteorol. Soc. Japan.* 75, 1041–1051.
- Fujibe, F., 2011. Urban warming in Japanese cities and its relation to climate change monitoring. *Int. J. Climatol.* 31:162–173. <http://dx.doi.org/10.1002/joc.2142>.
- Fujibe, F., 2012. Observational features of urban climates in Japan. *Meteorological Research Note (Kishio Kenkyu Note)* 224, 1–15 (in Japanese).
- Fujibe, F., Yamazaki, N., Katsuyama, M., Kobayashi, K., 2005. The increasing trend of intense precipitation in Japan based on four-hourly data for a hundred years. *SOLA* 1, 41–44.
- Fujibe, F., Togawa, H., Sakata, M., 2009. Long-term change and spatial anomaly of warm season afternoon precipitation in Tokyo. *SOLA* 5, 17–20.
- Gero, A.F., Pitman, A.J., 2006. The impact of land cover change on a simulated storm event in the Sydney Basin. *J. Appl. Meteorol. Climatol.* 45:283–300. <http://dx.doi.org/10.1175/JAM2337.1>.
- Grimmond, C. S. B., M. Blackett, M. J. Best, J. Barlow, J.-J. Baik, S. E. Belcher, S. I. Bohnenstengel, I. Calmet, F. Chen, A. Dandou, K. Fortuniak, M. L. Gouveia, R. Hamdi, M. Hendry, T. Kawai, Y. Kawamoto, H. Kondo, E. S. Krayenhoff, S.-H. Lee, T. Loridan, A. Martilli, V. Masson, S. Miao, K. Oleson, G. Pigeon, A. Porson, Y.-H. Ryu, F. Salamanca, L. Shashua-Bar, G.-J. Steeneveld, M. Tombrou, J. Voogt, D. Young, and N. Zhang, 2010: The international urban energy balance models comparison project: first results from phase 1. *J. Appl. Meteorol. Climatol.*, 49, 1268–1292.
- Haberlie, A.M., Ashley, W.S., Pingel, T.J., 2015. The effect of urbanisation on the climatology of thunderstorm initiation. *Q. J. R. Meteorol. Soc.* 141:663–675. <http://dx.doi.org/10.1002/qj.2499>.
- Hamdi, R., Degrauwe, D., Termonia, P., 2012. Coupling the town energy balance (TEB) scheme to an operational limited-area NWP model: evaluation for a highly urbanized area in Belgium. *Wea. Forecasting* 27, 323–344.
- Han, J.-Y., Baik, J.-J., Lee, H., 2014. Urban impacts on precipitation. *Asia-Pac. J. Atmos. Sci.* 50, 17–30.
- Hand, L.M., Shepherd, J.M., 2009. An investigation of warm-season spatial rainfall variability in Oklahoma City: possible linkages to urbanization and prevailing wind. *J. Appl. Meteorol. Climatol.* 48:251–269. <http://dx.doi.org/10.1175/2008JAMC2036.1>.
- Ikebuchi, S., Tanaka, K., Ito, Y., Moteki, Q., Souma, K., Yorozu, K., 2007. Investigation of the effects of urban heating on the heavy rainfall event by a cloud resolving model CReSiBUC. *Ann. Disaster Prev. Res. Inst., Kyoto Univ.* 50C, 105–111.
- Inamura, T., Izumi, T., Matsuyama, H., 2011. Diagnostic study of the effects of a large city on heavy rainfall as revealed by an ensemble simulation: a case study of central Tokyo, Japan. *J. Appl. Meteorol. Climatol.* 50, 713–728.
- Inoue, T., Kimura, F., 2004. Urban effects on low-level clouds around the Tokyo metropolitan area on clear summer days. *Geophys. Res. Lett.* 31, L05103. <http://dx.doi.org/10.1029/2003GL018908>.
- Inoue, T., Kimura, F., 2007. Numerical experiments on fair-weather clouds forming over the urban area in northern Tokyo. *SOLA* 3, 125–128.
- Ishizaki, N.N., Takayabu, I., Ohizumi, M., Sasaki, H., Dairaku, K., Iizuka, S., Kimura, F., Kusaka, H., Adachi, S.A., Kurihara, K., Murazaki, K., Tanaka, K., 2012. Improved performance of simulated Japanese climate with a multi-model ensemble. *J. Meteor. Soc. Japan* 90B, 235–254.
- Japan Meteorological Agency, 2014. Climate change monitoring report 2013. Available online at: http://www.jma.go.jp/jma/en/NMHS/index_ccmr.html (accessed May 26, 2016).
- Japan Meteorological Agency, 2015. Heat island monitoring report 2014. Available online at: <http://www.data.jma.go.jp/cpdinfo/himr/h27/index.html> (in Japanese, accessed May 26, 2016).
- Kanae, S., Oki, T., Kashida, A., 2004. Changes in hourly heavy precipitation at Tokyo from 1890 to 1999. *J. Meteor. Soc. Japan* 82, 241–247.
- Kanda, M., 2007. Progress in urban meteorology: a review. *J. Meteorol. Soc. Japan* 85B:363–383. <http://dx.doi.org/10.2151/jmsj.85B.363>.
- Kaufmann, R.K., Seto, K.C., Schneider, A., Liu, Z., Zhou, L., Wang, W., 2007. Climate response to rapid urban growth: evidence of a human-induced precipitation deficit. *J. Clim.* 20:2299–2306. <http://dx.doi.org/10.1175/JCLI4109.1>.
- Kishtawal, C.M., Niyogi, D., Tewari, M., Pielke Sr., R.A., Shepherd, J.M., 2010. Urbanization signature in the observed heavy rainfall climatology over India. *Int. J. Climatol.* 30, 1908–1916.
- Kitagawa, H., 2000. Radiation processes. *Sep. Vol. Annu. Rep. NPD* 46, 16–31 (in Japanese).
- Kug, J.-S., Ahn, M.S., 2013. Impact of urbanization on recent temperature and precipitation trends in the Korean peninsula. *Asia-Pac. J. Atmos. Sci.* 49, 151–159.
- Kusaka, H., Kondo, H., Kikegawa, Y., Kimura, F., 2001. A simple single-layer urban canopy model for atmospheric models: comparison with multi-layer and slab models. *Bound.-Layer Meteor.* 101, 329–358.
- Kusaka, H., Nawata, K., Suzuki-Parker, A., Takane, Y., Furuhashi, N., 2014. Mechanism of precipitation increase with urbanization in Tokyo as revealed by ensemble climate simulations. *J. Appl. Meteorol. Climatol.* 53, 824–839.
- Lin, C.-Y., Chen, W.-C., Liu, S.C., Liou, Y.A., Liu, G.R., Lin, T.H., 2008. Numerical study of the impact of urbanization on the precipitation over Taiwan. *Atmos. Environ.* 42, 2934–2947.
- Mashiko, W., Niino, H., Kato, T., 2009. Numerical simulation of tornadogenesis in an outer-rainband minisupercell of Typhoon Shanshan on 17 September 2006. *Mon. Weather Rev.* 137, 4238–4260.
- Masson, V., 2000. A physically-based scheme for the urban energy budget in atmospheric models. *Bound.-Layer Meteor.* 94, 357–397.
- Matheson, M.A., Ashe, Y., 2008. The effect of changes of urban surfaces on rainfall phenomenon as determined by a nonhydrostatic mesoscale model. *J. Meteor. Soc. Japan* 86, 733–751.
- Mitra, C., Shepherd, J.M., 2016. Urban precipitation: a global perspective. In: Seto, K.C., Solecki, W., Griffith, C.A. (Eds.), *The Routledge Handbook of Urbanization and Global Environment Change*. Taylor & Francis Group LLC, pp. 152–168.
- Mote, T.L., Lacke, M.C., Shepherd, J.M., 2007. Radar signatures of the urban effect on precipitation distribution: a case study for Atlanta, Georgia. *Geophys. Res. Lett.* 34:2–5. <http://dx.doi.org/10.1029/2007GL031903>.

- Nakanishi, M., Niino, H., 2006. An improved Mellor–Yamada level-3 model: its numerical stability and application to a regional prediction of advection fog. *Bound.-Layer Meteorol.* 119, 397–407.
- Niyogi, D., Holt, T., Zhong, S., Pyle, P.C., Basara, J., 2006. Urban and land surface effects on the 30 July 2003 mesoscale convective system event observed in the southern Great Plains. *J. Geophys. Res. Atmos.* 111:1–20. <http://dx.doi.org/10.1029/2005JD006746>.
- Niyogi, D., Pyle, P., Lei, M., Arya, S.P., Kishtawal, C.M., Shepherd, M., Chen, F., Wolfe, B., 2011. Urban modification of thunderstorms: an observational storm climatology and model case study for the Indianapolis urban region. *J. Appl. Meteorol. Climatol.* 50: 1129–1144. <http://dx.doi.org/10.1175/JAMC1836.1>.
- Oke, T.R., 1987. *Boundary Layer Climates*. second ed. Methuen 435pp.
- Pielke, R.A., Adegoke, J., Beltran-Przekurat, A., Hiemstra, C.A., Lin, J., Nair, U.S., Niyogi, D., Nobis, T.E., 2007. An overview of regional land-use and land-cover impacts on rainfall. *Tellus B* 59:587–601. <http://dx.doi.org/10.1111/j.1600-0889.2007.00251.x>.
- Rosenfeld, D., 2000. Suppression of rain and snow by urban and industrial air pollution. *Science* 287:1793–1796. <http://dx.doi.org/10.1126/science.287.5459.1793>.
- Rozoff, C.M., Cotton, W.R., Adegoke, J., 2003. Simulation of St. Louis Missouri, land use impacts on thunderstorms. *J. Appl. Meteorol.* 42, 716–738.
- Saito, K., 2012. The JMA nonhydrostatic model and its applications to operation and research. *Atmospheric Model Applications*:85–110 <http://dx.doi.org/10.5772/35368>.
- Saito, K., Fujita, T., Yamada, Y., Ishida, J., Kumagai, Y., Aranami, K., Ohmori, S., Nagasawa, R., Kumagai, S., Muroi, C., Kato, T., Eito, H., Yamazaki, Y., 2006. The operational JMA nonhydrostatic mesoscale model. *Mon. Weather Rev.* 134, 1266–1298.
- Saito, K., Ishida, J., Aranami, K., Hara, T., Segawa, T., Narita, M., Honda, Y., 2007. Nonhydrostatic atmospheric models and operational development at JMA. *J. Meteor. Soc. Japan* 86B, 271–304.
- Sato, T., Terashima, T., Inoue, T., Kimura, F., 2006. Intensification of convective precipitation systems over Tokyo urban area in summer season. *Tenki* 53, 479–484 (in Japanese with English abstract).
- Senoo, H., Kanda, M., Kinouchi, T., Hagishima, A., 2004. Estimation of anthropogenic heat and vapour emission, and the impact on local meteorology. *Ann. J. Hydr. Eng.* 48, 160–174 (in Japanese with English abstract).
- Shem, W., Shepherd, M., 2009. On the impact of urbanization on summertime thunderstorms in Atlanta: two numerical model case studies. *Atmos. Res.* 92, 172–189.
- Shepherd, J.M., 2005. A review of current investigations of urban-induced rainfall and recommendations for the future. *Earth Interact.*:9 <http://dx.doi.org/10.1175/EI156.1>.
- Shepherd, J.M., 2013. Impacts of urbanization on precipitation and storms: physical insights and vulnerabilities. In: Pielke, R. (Ed.), *Climate Vulnerability: Understanding and Addressing Threats to Essential Resources Volume 5*. Elsevier Inc., Academic Press, pp. 109–125.
- Shepherd, J.M., Pierce, H., Negri, A.J., 2002. Rainfall modification by major urban areas: observations from spaceborne rain radar on the TRMM satellite. *J. Appl. Meteorol.* 41, 689–701.
- Shimadera, H., Kondo, A., Shrestha, K.L., Kitaoka, K., Inoue, Y., 2015. Numerical evaluation of the impact of urbanization on summertime precipitation in Osaka, Japan. *Adv. Meteorol.* 2015:1–11. <http://dx.doi.org/10.1155/2015/379361>.
- Shimoji, R., Nakayoshi, M., Kanda, M., 2010. Case analyses of localized heavy rain in Kanto considering urban parameters. *Ann. J. Hydraul. Eng.* 54, 349–354 (in Japanese with English abstract).
- Souma, K., Tanaka, K., Suetsugi, T., Sunada, K., Tsuboki, K., Shinoda, T., Wang, Y., Sakakibara, A., Hasegawa, K., Moteki, Q., Nakakita, E., 2013. A comparison between the effects of artificial land cover and anthropogenic heat on a localized heavy rain event in 2008 in Zoshigaya, Tokyo, Japan. *J. Geophys. Res. Atmos.* 118:11,600–11,610. <http://dx.doi.org/10.1002/jgrd.50850>.
- Takahashi, H., Nakamura, Y., Suzuki, H., 2011. Frequency distribution of intense rainfall in the wards of Tokyo and its relationship with the spatial structure of building heights. *J. Geogr.* 120, 359–381 (in Japanese with English abstract).
- Trusilova, K., Jung, M., Churkina, G., Karstens, U., Heimann, M., Claussen, M., 2008. Urbanization impacts on the climate in Europe: numerical experiments by the PSU–NCAR mesoscale model (MM5). *J. Appl. Meteorol. Climatol.* 47, 1442–1455.
- United Nations, 2014. World Urbanization Prospects: The 2014 Revision, Highlights (ST/ESA/SERA/352). Department of Economic and Social Affairs, Population Division Available online at. <http://esa.un.org/unpd/wup> (accessed Feb. 15, 2016).
- Wang, J., Feng, J., Yan, Z., Hu, Y., Jia, G., 2012. Nested high-resolution modeling of the impact of urbanization on regional climate in three vast urban agglomerations in China. *J. Geophys. Res.* 117, D21103. <http://dx.doi.org/10.1029/2012JD018226>.
- Yabu, S., Murai, S., Kitagawa, H., 2005. Clear sky radiation scheme. *Sep. Vol. Annu. Rep. NPD* 51, 53–64 (in Japanese).
- Yang, L., Tian, F., Smith, J.A., Hu, H., 2014. Urban signatures in the spatial clustering of summer heavy rainfall events over the Beijing metropolitan region. *J. Geophys. Res. Atmos.* 119:1203–1217. <http://dx.doi.org/10.1002/2013JD020762>.
- Yonetani, T., 1982. Increase in number of days with heavy precipitation in Tokyo urban area. *J. Appl. Meteorol.* 21, 1466–1471.
- Yonetani, T., 1989. Study of the urban effects on the occurrence of convective precipitation. *Rep. Natl. Res. Cent. Disaster Prev.* 44, 1–59.
- Yoshikado, H., 1992. Numerical study of the daytime urban effect and its interaction with the sea breeze. *J. Appl. Meteorol.* 31, 1146–1164.
- Zhang, C.L., Chen, F., Miao, S.G., Li, Q.C., Xia, X.A., Xuan, C.Y., 2009. Impacts of urban expansion and future green planting on summer precipitation in the Beijing metropolitan area. *J. Geophys. Res.* 114, D02116. <http://dx.doi.org/10.1029/2008JD010328>.
- Zhang, Y., Smith, J.A., Luo, L., Wang, Z., Baeck, M.L., 2014. Urbanization and rainfall variability in the Beijing metropolitan region. *J. Hydrometeorol.* 15, 2219–2235.